Title
Using switchable mouse models to assess the therapeutic potential of MdmX and E2F3.

Author
Garcia, Daniel

Publication Date
2011

Peer reviewed|Thesis/dissertation

Using switchable mouse models to assess the therapeutic potential of MdmX and E2F3

by

Daniel Garcia

DISSERTATION

Submitted in partial satisfaction of the requirements for the degree of

DOCTOR OF PHILOSOPHY

in

Biomedical Sciences

in the

GRADUATE DIVISION

of the

UNIVERSITY OF CALIFORNIA, SAN FRANCISCO

[redacted]

DEDICATORIA

Esta obra está dedicada a mi esposa Wendy: nada de esto hubiera sido posible sin su apoyo incondicional. La dedico también a mis tres hijos, Santiago, Aldo y Andrés: ellos son la sonrisa al final del día y la razón de ser de mi trabajo.

ACKNOWLEDGMENTS

First and foremost, I would like to thank my graduate advisor, Gerard Evan, for allowing me to pursue doctoral studies in his lab. He has been a huge source of inspiration and has definitely pushed me to approach scientific problems in the most creative and innovative of ways. He was both patient and supportive as I matured as a scientist. He always made me think, and that has made me a better scientist.

I would like to thank the members of my thesis committee, Allan Balmain, Jay Debnath and Frank McCormick for all their time and attention throughout the many hard-to-schedule meetings of my PhD. Their enthusiastic, but critical look at my work and progress always prompted me to be better each time. Thanks for your support –and letters, of course.

I would like to thank the members of the Evan lab as well. Everyone was tremendously helpful and deserves credit for the completion of my PhD. A special thanks goes to Carla Martins, for letting me soak up all her expertise and for teaching me how to be a rigorous scientist. In many ways, I'm her first graduate student. Thanks also to Lamorna Swigart, without whom no Evan lab would exist. Thanks to my bench-mates Melissa Junttila and Debbie Burkhart for the day-to-day exciting discussions about our projects. I owe Laura Soucek, Nicole Sodir and Jony Whitfield many favors which I will never be able to pay back. Last, but not least, thanks to Fanya Rostker for her diligent management of our mouse colony.

I also need to thank our collaborators, whose contributions to my projects have been invaluable. In particular, I would like to thank Jackie Lees and Paul Danielian for their help in setting up the E2F3 project. Thanks also to Emmanuelle Passegué and Matt Warr for collaborating with me for the analysis of hematopoietic cells. Thanks to all the investigators that contributed with genetically engineered mice for my studies: Guillermina Lozano, Shaun Coughlin and Gustavo Leone.

One very special thanks for my classmate –and *compadre*- Jaime López and his family. Without ever meeting me before, he took me into his house when I first moved to San Francisco while I found a place for my family to stay. It was the beginning of a friendship that later made my family's stay in the Bay Area that more pleasant. We both were proudly "the Mexican guys" in the program.

Finally, my deepest thanks to my wife Wendy for her unconditional support. Pursuing my crazy dreams of becoming a scientist would not have been possible without her. Patience and love were always her gifts to me. Thanks to my sons, Santiago, Aldo and Andrés for their hugs and kisses every day I returned home from work. They gave me lots of sleepless nights, but it was all worth it.

ABSTRACT

Using switchable mouse models to assess the therapeutic potential of MdmX and E2F3

by

Daniel Garcia

Diverse as tumors are, they share some common features that are hallmarks of cancer. Two of these hallmarks are the evasion of tumor surveillance mechanisms and deregulated proliferation. Aiming to address these problems, we have used novel switchable mouse models to test the therapeutic potential of MdmX and E2F3, two genes directly involved in allowing tumor cells to evade tumor suppression and to proliferate, respectively.

MdmX is a critical negative regulator of p53 whose over-expression in many cancers is thought to block p53 tumor suppressor function. Consequently, inhibiting MdmX has emerged as an intriguing approach to restoring p53 function in established cancers. However, MdmX-deficient mice exhibit p53-dependent death early in embryogenesis, which has precluded elucidation of the consequences of systemic MdmX inhibition. To determine directly the effects of systemic MdmX inhibition in normal adult tissues and in tumors, we crossed *mdmX*$^{-/-}$ mice into the *p53ER*^{TAM} *knock-in* background to obtain adult MdmX-null mice in which p53 function can be restored. p53 became active when transiently restored in these mice, but the effects of this activity were non-lethal and

reversible. Moreover, absence of MdmX enhanced p53 restoration therapy in a mouse model of lymphoma. Hence, systemic inhibition of MdmX is a feasible therapeutic strategy for restoring p53 function in tumors that retain wild type p53.

The E2F family of transcription factors plays a key role in a number of cellular processes, including cellular proliferation and tumorigenesis. E2Fs are deregulated in the vast majority of cancer and appear to be essential conduits for upstream oncogenic lesions. Recent genetic studies in mice have established E2F3 as the most essential activating E2F for cellular proliferation and embryonic viability. However, the embryonic lethality of E2F3-null mice has prevented the study of the contribution of E2F3 to tumor proliferation and the assessment of E2F3 inhibition as a therapeutic avenue. To directly study E2F3 biology in adult tissues and tumors, we established a novel tet-repressor system that allows control of endogenous *e2f3* expression in adult mice.

TABLE OF CONTENTS

LIST OF FIGURES

Chapter 1

Introduction

Diverse as tumors are, they share some common features that are hallmarks of cancer (Hanahan and Weinberg 2000). Effective therapeutic strategies that are truly cancer specific must necessarily tackle these hallmarks that set cancer cells apart from normal cells. Two of these hallmarks are the evasion of tumor surveillance mechanisms and deregulated proliferation. Genes and pathways that play a major role in these features have become increasingly clear, as have new potential targets that might generate cancer-specific therapies. With that objective in mind, we have used novel switchable mouse models to test the therapeutic potential of MdmX and E2F3, two genes directly involved in allowing tumor cells to evade tumor suppression and to proliferate, respectively.

Modeling MdmX inhibition.

The p53 transcription factor coordinates responses in somatic cells to a variety of stresses, including DNA damage, hypoxia and oncogene activation, by triggering growth arrest or cell death of the damaged cell. The pivotal role that p53 plays in tumor suppression is evidenced by the fact that the p53 pathway is functionally inactivated in the majority of human cancers and that p53-deficient mice develop cancer at high frequencies (Vousden and Lane 2007; Kruse and Gu 2009). Intriguingly, many cancers retain expression of wild type p53, inactivating instead upstream or downstream p53 pathway components, and intense research has focused on finding ways to reactivate p53 function selectively in such p53-competent tumors. Hitherto, most pharmacological

strategies have sought to inhibit Mdm2, a critical negative regulator of p53 (Issaeva et al. 2004; Vassilev et al. 2004; Shangary et al. 2008; Sun et al. 2008; Vazquez et al. 2008; Canner et al. 2009; Hedstrom et al. 2009). While such studies confirm that inhibition of Mdm2 can activate latent p53 in tumor cells, it also triggers pathological p53 function in normal tissues (Boesten et al. 2006; Francoz et al. 2006; Grier et al. 2006; Ringshausen et al. 2006; Xiong et al. 2006; Maetens et al. 2007; Valentin-Vega et al. 2008), narrowing the therapeutic window available for Mdm2 inhibition in cancer therapy.

MdmX, also known as Mdm4, has recently emerged as a discrete critical negative regulator of p53 (Mancini et al., 2010; Marine and Jochemsen, 2005; Marine et al., 2007; Wade and Wahl., 2009). While MdmX is structurally related to Mdm2, it does not target p53 for degradation via ubiquitin ligation but, instead, acts as a direct transcriptional squelcher of p53 (Marine and Jochemsen 2005; Marine et al. 2007; Kruse and Gu 2009; Wade and Wahl 2009). MdmX also modulates Mdm2 stability and function, thereby indirectly regulating p53 (Jackson et al. 2001; Uldrijan et al. 2007; Linke et al. 2008; Okamoto et al. 2009). Like Mdm2, MdmX is overexpressed in many cancers, especially those of breast, colon, lung, as well as in glioma, lymphoma and retinoblastoma (Danovi et al. 2004; Laurie et al. 2006), where it is thought to promote tumorigenesis by suppressing p53 function. However, knockout (Parant et al. 2001; Migliorini et al. 2002) and conditional deletion studies (Francoz et al. 2006; Grier et al. 2006; Xiong et al. 2006) have also shown that MdmX, like Mdm2, is required as a continuous buffer against precocious p53 activity during development of normal

tissues. Whether MdmX inhibition also shares the same disquieting toxicity in adult tissues as does Mdm2 inhibition has been confounded by this embryonic lethality of p53-competent *mdmX* knockout mice, as has evaluation of the utility of MdmX inhibition in cancer therapy.

To model directly the side effects of systemic MdmX inhibition in adult animals together with the therapeutic potential of MdmX inhibition in tumors, we crossed *mdmX*$^{+/-}$ mice with *p53ER*^{TAM} *knock-in* (*p53*^{KI}) animals. *p53*$^{KI/KI}$ mice express a 4-hydroxy-tamoxifen (4-OHT) dependent variant of endogenous p53 in place of the wild type protein and are effectively p53-deficient in the absence of 4-OHT ligand and p53 wild type in its presence (Christophorou et al. 2005). p53 function was then systemically restored in adult *mdmX*$^{-/-}$;*p53*^{KI} mice. We here show that MdmX, like Mdm2, is indeed continuously required to suppress untoward p53 function in adult tissues and their stem cells. However, unlike even fleeting p53 function in *mdm2*$^{-/-}$ mice, which is rapidly and ineluctably fatal, transient p53 function is well tolerated by *mdmX*$^{-/-}$ animals. We show that Mdm2 remains functional in the absence of MdmX, which likely explains the milder effects of p53 restoration in *mdmX*$^{-/-}$ mice compared with restoration in *mdm2*$^{-/-}$ mice. Moreover, absence of MdmX potentiates the therapeutic benefit of p53 restoration in a lymphoma model. These data intimate that inhibition of MdmX would be an effective therapeutic strategy for restoring p53 function in cancer that is better tolerated than is inhibition of Mdm2.

Modeling E2F3 inhibition.

The E2F family of transcription factors plays a key role in a number of cellular processes. E2Fs were first shown to control the cell cycle dependent expression of genes that are essential for cellular proliferation, especially components of DNA replication machinery (Wu et al. 2001) (DeGregori 2002). Since then, E2Fs have been implicated in other processes like apoptosis, DNA damage response and tumorigenesis, both as tumor suppressors and oncogenes (McClellan and Slack 2007; Polager and Ginsberg 2009). E2Fs interact with components of key tumor suppressor pathways, like the Rb and ARF/p53 pathways, and are therefore predicted to be deregulated in the vast majority of cancers (Rowland et al. 2002; Sherr and McCormick 2002; Chen et al. 2009). Interestingly, E2Fs are never themselves mutated in cancers and appear to be instead essential conduits for upstream oncogenic lesions. There are eight identified members of the E2F family, which can be divided into activators of transcription, E2F1-3 (E2F3 has two isoforms, E2F3a and E2F3b), and repressors of transcription, E2F4-8. This division has recently come into question, however, as E2F activators were found to function as repressors in differentiating cells (Chong et al. 2009). Together, E2F transcription factors establish a complex regulation of more than 130 known target genes that function to initiate S phase, DNA synthesis, DNA repair and mitosis (Bracken et al. 2004).

The *e2f3* gene encodes two proteins, E2F3a and E2F3b (Leone et al. 2000). Each is under the control of distinct promoters, with distinct patterns of

expression. E2F3a follows a cell cycle controlled expression pattern similar to activators E2F1 and E2F2, with maximum expression at the beginning of S phase (Adams et al. 2000). Accordingly, E2F3a is an E2F and Myc target gene. E2F3b, on the other hand, is not dependent on the cell cycle and has a constant level of expression, similar to E2F4 and E2F5 (Adams et al. 2000). Each E2F3a and E2F3b has its own distinct exon 1 (named exon 1a and exon 1b, respectively), but share all other exons. E2F3b is, in effect, a truncated form of E2F3a, missing the cyclin-A binding site believed to have a role in the downregulation of E2F3a at the end of S phase. Knockout mice have been generated for all activating E2Fs, with E2F3 knockout mice displaying the most severe phenotype (Humbert et al. 2000; Wu et al. 2001; Cloud et al. 2002). E2F3 knockout mouse embryonic fibroblasts (MEFs) have a slower cell cycle rate and show reduced expression of E2F target genes. Contrary to E2F1 and E2F2 deficiencies (even E2F1;E2F2 double knockout mice), which yield viable mice, E2F3 deficiency is mostly embryonic lethal, with the only a few surviving mice dying as juveniles from heart failure (Humbert et al. 2000; Cloud et al. 2002; King et al. 2008). E2F3a and E2F3b single knockouts are viable, demonstrating that both proteins can compensate for each other *in vivo* (Danielian et al. 2008; Chong et al. 2009). Further studies have now shown that E2F3a alone can support full embryonic development. Interestingly, it is the E2F3a promoter and not the protein that is essential for development, as knocking in E2F1 in the *e2f3a* locus also supported full development (Tsai et al. 2008). On top its critical role in proliferation and development, recent evidence has increasingly

implicated E2F3 in cancer. E2F3 is overexpressed in bladder cancer (Feber et al. 2004), retinoblastoma (Grasemann et al. 2005), prostate (Foster et al. 2004) and its expression has been associated with increased cancer aggressiveness (Ziebold et al. 2003; Foster et al. 2004). In addition, recent evidence also implicates E2F3 in apoptosis as well (Ziebold et al. 2003; Paulson et al. 2006), for example after DNA damage (Martinez et al., 2010). Furthermore, there is evidence that E2F3 interacts with ARF, a key tumor suppressor (Paulson et al. 2006) (Aslanian et al. 2004). E2F3b represses ARF in quiescent MEFs, whereas E2F3a activates ARF transcription only upon sustained growth stimulation (Aslanian et al. 2004). However, how E2F3 actually regulates ARF in the adult mouse or in tumors is not known. Despite these advances, our understanding of E2F3 biology in vivo remains very poor, especially in adult animals, mainly because of the embryonic lethality of E2F3-null mice. To study E2F3 biology in adult tissues and tumors, we have implemented a novel genetic model that allows us to grow mice in which E2F3 expression can be repressed in adulthood via the use of a tetracycline sensitive repressor.

The tet-repressor system.

Classical approaches to manipulating genes in mice include generation of knockout or transgenic animals (Gossen and Bujard 2002). Despite their proven usefulness, application of these classical approaches to genes essential for embryonic development, like the *e2f3* gene, suffers several intrinsic problems. First, embryonic lethality of *e2f3*-knockout mice (Cloud et al. 2002) prevents any

study of E2F3 function in the adult animal, thus restricting analysis of E2F3 biology to early developmental stages or to in vitro studies. Even so, developmental compensation may confound observed phenotypes. Moreover, a substantial disadvantage of the *e2f3*-knockout approach is its irreversibility, which limits the questions that can be addressed. Second, E2F3 transgenic mouse models (Paulson et al. 2006) depend on overexpression, resulting in a phenotype that does not reflect normal E2F3 biology. More importantly, E2F3 transgenic mice fail to recapitulate the complex regulation of the *e2f3* locus, in particular, the differential regulation of E2F3a and E2F3b. For some genes, addition of estrogen receptor (ER) modules (or other regulatable moieties) to the endogenous gene has solved many of the problems posed by knockout and transgenic approaches (Christophorou et al. 2005). However, an ER approach cannot be applied to genes essential for development because ER inducers are abortive. Application of a novel tet-repressor system to the *e2f3* gene solves these problems.

The tet-repressor system is a novel genetic approach that utilizes previously established components of the tTA expression system, but uses the tetracycline sensitive repressor tTS (tetracycline-Trans-Silencer) as the molecular switch (Freundlieb et al. 1999), instead of the tetracycline sensitive transactivators tTA and rtTA. The system consists in the insertion of a 300 base pair evolutionary distant prokaryotic DNA element that contains seven tet operator (tet^{o}) sequences, called TRE (for Tet-Responsive-Element), into an otherwise untouched endogenous gene. The TRE sequence functions as a

binding site for the tTS dominant transcriptional repressor. The tTS repressor, also referred to as tTS^{kid1}, comprises a modified tetracycline sensitive DNA binding domain fused to the transcriptional silencing KRAB domain of the Kid-1 protein (Freundlieb et al, 1999). The KRAB domain represses transcription by changing local chromatin structure (Ryan et al. 1999). The tTS repressor displays very low basal activity, good inducibility and has successfully been used to control gene expression in transgenes (Lamartina et al. 2003). tTS can be exogenously and reversibly controlled by non-toxic compounds like doxycycline or tetracycline, effectively functioning as a molecular switch. In the absence of doxycycline, tTS dimerizes and binds the TRE sequence to block transcription of the nearby gene. Addition of doxycycline makes tTS inactive and releases it from the TRE, allowing normal transcription to ensue (Figure 1-1). Importantly, the tet-repressor system does not result in overexpression or activation of the target gene: the switch is from no expression to *normal* expression of the gene. Thus, this tet-repressor system allows ectopic and temporal control of the gene of interest in its endogenous context.

We have now successfully applied this novel technology to the *e2f3* gene and have generated mice with a TRE insertion in the *e2f3* locus ($e2f3^{tre}$ allele). Insertion of the TRE sequence did not disrupt normal *e2f3* transcription. We have crossed these $e2f3^{tre}$ mice to a transgenic mouse line that expresses the tTS repressor from the β-actin promoter. We show that tTS efficiently and reversibly represses *e2f3* transcription in $e2f3^{tre/tre}$*;tTS* MEFs and $e2f3^{tre/tre}$*;tTS* mice in the absence of doxycycline. Moreover, this system permits normal *e2f3* expression

during development, thus avoiding embryonic lethality and compensation, and allows us to block its transcription in adult tissues and tumors. As a result and for the first time ever, tet-repressor targeting of *e2f3* allowed us to systemically remove during adulthood a gene that is essential for embryonic development. We show that E2F3 is dispensable for adult viability, however, repression of *e2f3* was not therapeutically beneficial in a mouse model of lymphoma. Importantly, beyond our studies on E2F3 biology, validation of the tet-repressor system has enormous implications for the future of mouse genetics.

FIGURE LEGENDS

Figure 1-1. Model for tet-repressor targeting.

A) In the presence of doxycycline the tTS repressor is inactive and does not bind nor represses TRE-targeted alleles.

B) In the absence of doxycycline the tTS repressor dimerizes and becomes active, which allows it to bind and repress TRE-targeted alleles.

Figure 1-1

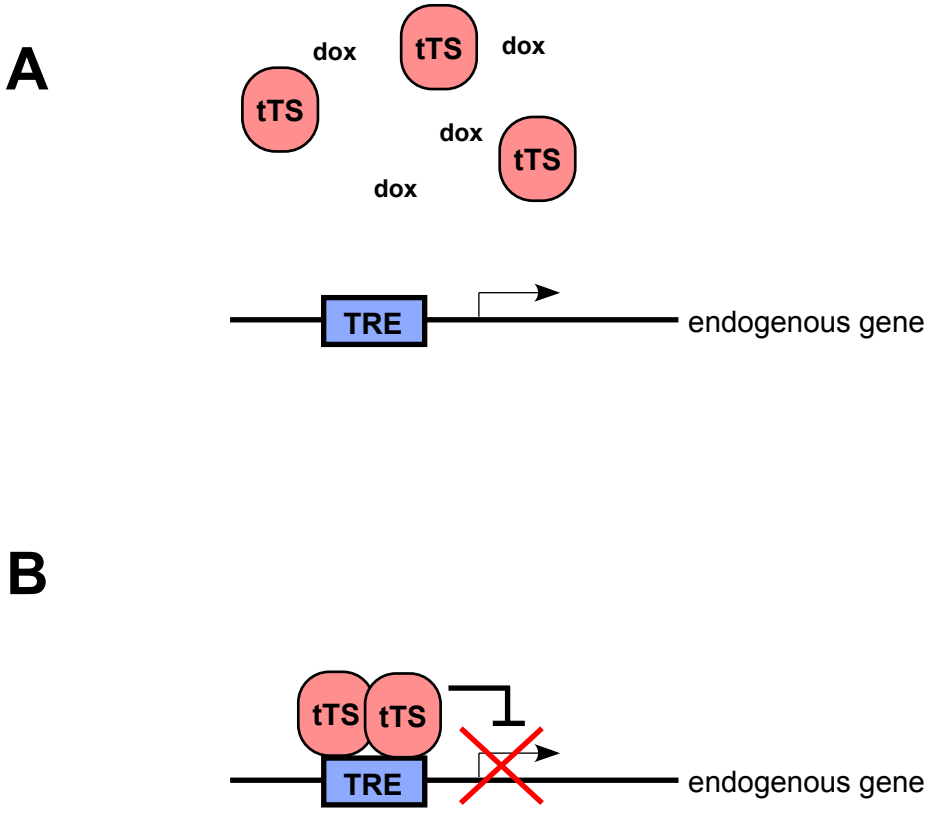
A
dox
tTS
dox
tTS
dox
tTS
dox
TRE
endogenous gene
B
tTS
tTS
TRE
endogenous gene

CHAPTER 2

Validation of MdmX as a therapeutic target to restore p53 function in tumors

p53 is spontaneously active in adult tissues in the absence of MdmX

To determine the extent to which MdmX restrains p53 activity in normal adult mouse tissues, we crossed *p53*$^{KI/KI}$ mice with *mdmX*$^{+/-}$ mice. No pups harboring two copies of the *p53*^{KI} allele were born in an *mdmX*$^{-/-}$ background indicating that, as reported with *mdm2*$^{-/-}$;*p53*$^{KI/KI}$ mice, even in the absence of 4-OHT there is some residual p53 activity in *mdmX*$^{-/-}$ mice from two copies of p53ER^{TAM} that is sufficient to induce embryonic lethality. However, *mdmX*$^{-/-}$ mice harboring only a single *p53ER*^{TAM} allele (*p53*$^{KI/-}$) were born at expected Mendelian ratios (as were *mdmX*$^{+/+}$;*p53*$^{KI/-}$ and *mdmX*$^{+/-}$;*p53*$^{KI/-}$ animals), indicating no biologically significant leakiness from a single copy of p53ER^{TAM}: consequently, *mdmX*$^{-/-}$;*p53*$^{KI/-}$ animals were used in all subsequent experiments.

To ascertain the extent of spontaneous p53 activity in adult tissues in the absence of MdmX, p53 was restored in *mdmX*$^{-/-}$;*p53*$^{KI/-}$ mice by systemic administration of tamoxifen and selected organs harvested for analysis 6 hours later. For direct evidence of p53 activity in the absence of MdmX, we assayed for the expression of known p53-target genes *cdkn1a* (encoding the Cdk inhibitor p21^{cip1}) and *puma* (encoding the pro-apoptotic BH3 protein PUMA). We noted rapid and dramatic induction of p53 target genes in tissues of tamoxifen-treated *mdmX*$^{-/-}$;*p53*$^{KI/-}$ mice confirming that p53 is, indeed, spontaneously active in adult tissues of MdmX-deficient mice (Figure 2-1A). However, quite unlike the situation following p53 functional restoration in the absence of Mdm2 (Ringshausen et al. 2006), where both *cdkn1a* and *puma* are profoundly induced in all tissues irrespective of whether or not that specific tissue then undergoes apoptosis,

restoration of p53 function in *mdmX*$^{-/-}$;*p53*$^{KI/-}$ tissues elicited more specific p53 target gene induction. While, with the exception of small intestine, p53 restoration potently induced *cdkn1a* in all tested tissues, the pro-apoptotic gene *puma* was induced only in classically radiosensitive tissues (spleen, thymus and intestinal epithelium) (Figure 2-1A).

This unexpected selectivity of p53 target gene induction in different *mdmX*$^{-/-}$ tissues was broadly mirrored by the biological outcomes of p53 restoration. Radiosensitive tissues (bone marrow, thymus, spleen and intestinal epithelium) of tamoxifen-treated *mdmX*$^{-/-}$;*p53*$^{KI/-}$ mice exhibited a marked increase in apoptosis compared to controls (*mdmX*$^{+/+}$;*p53*$^{KI/-}$ and *mdmX*$^{-/-}$;*p53*$^{-/-}$ mice treated with tamoxifen, or *mdmX*$^{-/-}$;*p53*$^{KI/-}$ mice treated with oil) (Figure 2-1B and data not shown). By contrast, no detectable apoptosis was observed in classically radio-resistant tissues like liver, kidney, lung and heart (Figure 2-1B and data not shown). Of note, despite the crucial role played by MdmX inhibition of p53 during development of the cerebellum, especially with regard to suppression of p53-dependent apoptosis in post-mitotic cerebellar neurons in embryos (Francoz et al. 2006), we saw no apoptosis or any other evident impact of p53 restoration on histology or cell viability in the fully formed adult cerebellum of *mdmX*$^{-/-}$ mice, even though significant p53 activity was evident from the induction of *cdkn1a* (Figure 2-2). p53-induced apoptosis was evident only in the continuously proliferating sub ventricular zones of *mdmX*$^{-/-}$;*p53*$^{KI/-}$ mouse brains (Figure 2-2).

mdmX$^{-/-}$ mice survive transient p53 restoration

Substantial evidence indicates that both Mdm2 and MdmX are crucial for reining in the toxic effects of untoward p53 activity. Indeed, we previously showed that even very transient restoration of p53 (i.e. a single tamoxifen injection) is lethal to adult Mdm2-deficient mice within 6 days (Ringshausen et al. 2006). In stark contrast, even 7 days sustained (i.e. daily tamoxifen injections) p53 restoration was not lethal to MdmX-deficient mice (Fig 2-3A), even though histological analysis indicated significant degenerative tissue-specific pathologies including striking suppression of proliferation and decreased cellularity in the bone marrow and red pulp of the spleen together with loss of structural integrity in the thymus (Figure 2-3B). Unexpectedly, given that intestines of tamoxifen-treated *mdm2*$^{-/-}$;*p53*$^{KI/-}$ mice rapidly succumb to severe and irreparable damage (Figure 2-4 and Ringshausen et al. 2006), intestinal epithelia of tamoxifen-treated *mdmX*$^{-/-}$;*p53*$^{KI/-}$ mice maintained normal architecture and barrier function throughout the 1 week of p53 restoration despite significant ongoing levels of p53-dependent apoptosis (that *en passant*, provide *de facto* evidence that restored p53 function is indeed maintained throughout the 7 days of tamoxifen treatment) (Figure 2-3C). One reason for the sustained structural integrity of *mdmX*$^{-/-}$ intestinal epithelia may be that proliferation in *mdmX*$^{-/-}$ intestines continues throughout p53 restoration (Figure 2-3C), a surprising observation that is nonetheless consistent with the failure of p53 to induce p21^{cip1} in that tissue (Figure 2-1A).

To ascertain whether *mdmX*$^{-/-}$ mice might survive permanent p53 restoration, *mdmX*$^{-/-}$;*p53*$^{KI/-}$ mice were treated daily with tamoxifen and their health and viability monitored. Long-term sustained p53 restoration was eventually lethal to *mdmX*$^{-/-}$ mice (Figure 2-5A, median survival of 29 days), albeit greatly delayed relative to the rapid demise (6 days) that succeeds p53 restoration in *mdm2*$^{-/-}$ mice. At the time of death, bone marrow, spleen and thymus of tamoxifen-treated *mdmX*$^{-/-}$;*p53*$^{KI/-}$ mice exhibited severe attrition, with decreased cellularity and loss of architectural integrity, reminiscent of that accompanying the far more rapid deaths of tamoxifen-treated *mdm2*$^{-/-}$;*p53*$^{KI/-}$ mice (Figure 2-5B). Once again, however, the dramatic loss of intestinal epithelial integrity that p53 restoration elicits in *mdm2*$^{-/-}$ animals (Figure 2-4 and Ringshausen et al. 2006) was absent from *mdmX*$^{-/-}$ animals: overall integrity of both the small and large intestines of *mdmX*$^{-/-}$;*p53*$^{KI/-}$ mice, as well as villus/crypt structure and ratio, were maintained even after long-term (26 days) sustained p53 restoration (Figure 2-5C). Detailed histological analysis of such intestines indicated an abnormal expansion of Paneth cells in the crypts and the concurrence of both sustained intestinal crypt proliferation (again, consistent with the absence of p21^{cip1} induction in intestines) and apoptosis (Figure 2-5C). Given this long-term maintenance of intestinal integrity in tamoxifen-treated *mdmX*$^{-/-}$;*p53*$^{KI/-}$ mice, the most plausible cause of their eventual demise is bone marrow failure: indeed, 26 day tamoxifen-treated *mdmX*$^{-/-}$ mice were severely anemic (reduced red blood cell count, reduced hemoglobin and hematocrit) and exhibited overall reduction of blood counts (Figure 2-6).

The pathologies induced by transient p53 activity in the absence of MdmX are fully reversible

To ascertain whether transient p53 restoration in *mdmX*$^{-/-}$ mice elicits irreversible damage in tissues, p53 was continuously restored in *mdmX*$^{-/-}$;*p53*$^{KI/-}$ mice for 7 days (daily injections) and tamoxifen then withdrawn to assess the capacity of tissues to regenerate. All affected tissues (bone marrow, spleen, thymus, intestine) recovered, appearing completely normal after one week: proliferation resumed in lymphoid organs (Figure 2-7A) and apoptosis declined in intestinal epithelia (Figure 2-7B). Thereafter, such mice lived long-term and exhibited no adverse consequences of transient systemic p53 activation. Hence, the extended survival of transiently tamoxifen-treated *mdmX*$^{-/-}$;*p53*$^{KI/-}$ (relative to *mdm2*$^{-/-}$ mice) is accompanied by greatly enhanced capacity to recover from the depredations of p53 restoration.

One possible explanation for both the maintenance of intestinal integrity and the expeditious recovery from p53 restoration in tamoxifen-treated *mdmX*$^{-/-}$;*p53*$^{KI/-}$ compared with tamoxifen-treated *mdm2*$^{-/-}$;*p53*$^{KI/-}$ animals is that the stem cell populations required to regenerate damaged tissues are less debilitated by the absence of MdmX than of Mdm2. To test this directly, we turned to the hematopoietic system in which the stem cell population is relatively well-characterized. Bone marrow cells were isolated from tamoxifen-treated *mdmX*$^{-/-}$;*p53*$^{KI/-}$ and *mdm2*$^{-/-}$;*p53*$^{KI/-}$ mice, immunostained, and hematopoietic stem cell (HSC) and mature cell compartments quantitated by flow cytometry. In agreement with our previous data (Ringshausen et al. 2006), p53 restoration in

mdm2-null mice triggered dramatic loss of total bone marrow cellularity within only one day: by 5 days, the bone marrow had been essentially annihilated - only a few hundred cells (1655.3 ± 558.2) were recoverable, making it impossible to conduct meaningful analysis of stem cells or other hematopoietic lineages at this or later time points (Figure 2-8A). By contrast, one day of p53 restoration in *mdmX*$^{-/-}$;*p53*$^{KI/-}$ mice elicited only a modest reduction in total bone marrow cellularity, although cell loss progressively continued as p53 activity was maintained over the succeeding week (Figure 2-8A). Control *mdmX*$^{-/-}$;*p53*$^{KI/-}$ mice not treated with tamoxifen maintained similar cell counts to tamoxifen-treated *mdmX*$^{+/+}$;*p53*$^{KI/-}$ mice (data not shown). Direct quantitation of HSCs (Lin-, Sca1^{+}, CD150^{+}, CD48^{-}) (Kiel et al. 2005), indicated that they are effectively ablated in *mdm2*$^{-/-}$;*p53*$^{KI/-}$ mice after only one day of p53 restoration (Figure 2-8B). By comparison, even though they are significantly decreased in number compared to wild type controls, more HSCs can be recovered from tamoxifen-treated *mdmX*$^{-/-}$;*p53*$^{KI/-}$ mice after 7 days of sustained p53 restoration than from 1 day-treated *mdm2*$^{-/-}$;*p53*$^{KI/-}$ animals (Figure 2-8B). Hence, the hematopoietic system can recover from short-term inactivity of MdmX but not of Mdm2. In conclusion, while both Mdm2 and MdmX are required for the long-term maintenance of HSCs in the presence of functional p53, it is clear that Mdm2 is the most exigent restraint to p53 toxicity.

Of note, sensitivity to p53 restoration in the absence of MdmX varied between different mature cell compartments. Myeloid cellularity in the bone marrow was unaffected even after 7 days of p53 restoration (Figure 2-8C)

whereas B-cells were very sensitive (Figure 2-8D). In all mature hematopoietic lineages, p53 activity in the absence of Mdm2 elicited far more dramatic and rapid cell attrition than in absence of MdmX, including mature cells in the spleen (Figure 2-9).

Mdm2 restrains p53 activity even when MdmX is absent, blunting the pathological impact of MdmX deficiency

Why should p53 be less toxic in the absence MdmX than without Mdm2? It is well established that p53 and Mdm2 form a negative feedback loop wherein active p53 induces expression of Mdm2 that, in turn, down-regulates p53 (reviewed in Kruse and Gu 2009). We hypothesized that, even in the absence of functional MdmX, Mdm2 can still restrain excessive p53 activity, thereby mitigating p53 toxicity. To test this, we took advantage of our switchable $p53^{KI/KI}$ model in which the engagement of the p53-Mdm2 negative feedback loop can be followed in real time. We previously showed that upon acute p53 restoration, p53 levels fall progressively – a down-regulation that is compromised in the absence of Mdm2 (Ringshausen et al. 2006). To determine whether p53 is down-regulated by Mdm2 in the absence of MdmX, we isolated $mdmX^{+/+}$;$p53^{KI/-}$ and $mdmX^{-/-}$;$p53^{KI/-}$ mouse embryonic fibroblasts (MEFs) and treated them with 4-OHT in the presence or absence of the Mdm2 inhibitor Nutlin-3a (Vassilev et al. 2004). As expected, p53 is down-regulated over time in 4-OHT-treated $mdmX^{+/+}$;$p53^{KI/-}$ MEFs. Also as expected, p53 is inactive without 4-OHT. However, following addition of 4-OHT, p53 function is restored and p53 activity

rises, as evidenced by the induction of p21^{cip1}. The decline in p53 level is partially abrogated when the *mdmX*$^{+/+}$;*p53*$^{KI/-}$ MEFs are co-treated with Nutlin-3a, demonstrating that Mdm2, at least in part, contributes to the eventual down-regulation of p53 level and activity in 4-OHT-treated *mdmX*$^{+/+}$ cells (Figure 2-10A). Similarly, p53 levels drop in *mdmX*$^{-/-}$;*p53*$^{KI/-}$ MEFs after addition of 4-OHT with concomitant increase in p53 activity. This p53 down-regulation is also inhibited by Nutlin-3a, resulting in yet higher p53 activity (Figure 2-10A), which demonstrates that Mdm2 contributes significantly to the down-regulation of p53 levels and activity even in the absence of MdmX.

To test whether Mdm2 also restrains p53 level and activity in *mdmX*$^{-/-}$ tissues *in vivo*, we treated *p53*$^{KI/-}$, *mdmX*$^{-/-}$;*p53*$^{KI/-}$, and *mdm2*$^{-/-}$;*p53*$^{KI/-}$ mice for one day with either vehicle or tamoxifen to restore p53 and monitored p53 levels over time in liver. As predicted, p53 levels dropped in the livers of *p53*$^{KI-}$ mice after p53 restoration, with little increase in p53 activity (measured by induction of *cdkn1a* mRNA) (Figure 2-10B). p53 levels also dropped after p53 restoration in livers of tamoxifen-treated *mdmX*$^{-/-}$;*p53*$^{KI/-}$ mice, albeit not as efficiently, consistent with a previously reported role of MdmX in the regulation of p53 protein levels (Gu et al. 2002; Okamoto et al. 2009). Nonetheless, despite this fall in overall p53 levels, p53 activity was induced in the absence of MdmX, as evidenced by a clear increase in *cdkn1a* (Figure 2-10B). Of note, *Mdm2* was also induced in *mdmX*$^{-/-}$;*p53*$^{KI/-}$ livers after tamoxifen administration, where it presumably contributes to p53 down-regulation (Figure 2-10B). In contrast, after p53 restoration in *mdm2*$^{-/-}$;*p53*$^{KI/-}$ livers p53 levels fail to drop and, indeed,

increase, resulting in even higher p53 activity (evidenced by robust induction of *cdkn1a*) (Figure 2-10B). Similar dynamics were observed in spleen, thymus and small intestine (data not shown). Overall, the stark differences in the down-regulation of p53 after restoration in organs of *mdmX*$^{-/-}$ versus *mdm2*$^{-/-}$ mice affirms that, even in the absence of MdmX, Mdm2 retains functionality and contributes to the mitigation of p53 levels and activity *in vivo*. Taken together, the persistence of the p53-Mdm2 negative feedback loop in *mdmX*$^{-/-}$ cells and tissues offers the most plausible explanation for the unexpectedly mild and recoverable impact of p53 in the absence of MdmX.

The therapeutic impact of restoring p53 in tumors is augmented by inactivation of MdmX

Several studies have shown that restoring p53 function in tumors is therapeutically beneficial (Junttila et al. 2010; Martins et al. 2006; Ventura et al. 2007; Xue et al. 2007). Since our data establish that transient p53 restoration in MdmX-deficient mice has only limited and delayed toxicity, we asked whether the absence of MdmX offers a useful therapeutic window with which to enhance the therapeutic benefit of restoring p53 in tumors *in vivo*. We crossed *mdmX*$^{-/-}$;*p53*$^{KI/-}$ mice to the lymphoma-prone *Eμ-Myc* transgenic strain (Adams et al. 1985). Tumors from *mdmX*$^{+/+}$;*p53*$^{KI/-}$;*EμMyc* and *mdmX*$^{-/-}$;*p53*$^{KI/-}$;*EμMyc* mice were then isolated and transplanted into multiple wild type recipients. Ten days after transplantation, recipient mice were treated for one week with either vehicle or tamoxifen. Consistent with our previous study (Martins et al. 2006), tamoxifen

treatment significantly extended the life-span of mice harboring *mdmX*$^{+/+}$;*p53*$^{KI/-}$;*Eμ-Myc* tumors compared with sham-treated controls (Figure 2-11). Vehicle-treated mice bearing *mdmX*$^{-/-}$;*p53*$^{KI/-}$;*Eμ-Myc* tumors showed no increase in overall survival relative to vehicle-treated MdmX-proficient controls, demonstrating that absence of MdmX alone does not affect tumor growth *per se*. However, p53 restoration in the absence of MdmX significantly increased overall survival relative to tamoxifen-treated *mdmX*$^{+/+}$;*p53*$^{KI/-}$;*Eμ-Myc* controls (Figure 2-11). Hence, p53 restoration in the absence of MdmX confers a significant therapeutic benefit over p53 restoration in its presence.

p53 restoration therapy in *Eμ-Myc* tumors is eventually compromised by the emergence of resistant tumor clones harboring additional mutations in the p53 pathway (Martins et al. 2006). To investigate if this is still a significant limitation even when p53 is restored in the absence of MdmX, we harvested tumors from treated host mice and cultured them *in vitro* in the presence or absence of 4-OHT. Tumor cells derived from vehicle-treated mice were rapidly killed when exposed to 4-OHT, regardless of MdmX genotype, indicating that absence of MdmX alone does not promote outgrowth of resistant clones (Figure 2-12A). By contrast, *mdmX*$^{+/+}$ and *mdmX*$^{-/-}$ tumor cells isolated from relapsed tamoxifen-treated mice survived and grew in the presence of 4-OHT, confirming that p53 restoration does indeed still select for resistant clones irrespective of MdmX status (Figure 2-12A).

Resistance to p53 restoration arises in *Eμ-Myc* tumors by either loss of p53 itself or by loss of p19^{ARF}, the essential upstream conduit for oncogenic

activation of p53 (Zindy et al. 2003; Martins et al. 2006). To establish the mechanism of acquired resistance to p53 restoration in MdmX-deficient tumors, we determined the status of p53 and $p19^{ARF}$ expression in transplanted *mdmX*$^{+/+}$;*p53*$^{KI/-}$;*EμMyc* and *mdmX*$^{-/-}$;*p53*$^{KI/-}$;*EμMyc* tumors. Tumors from vehicle-treated recipients all exhibited high $p19^{ARF}$ and readily detectable levels of p53, regardless of MdmX genotype. By contrast, *mdmX*$^{+/+}$;*p53*$^{KI/-}$;*EμMyc* tumors from tamoxifen-treated recipients had high $p19^{ARF}$ levels but substantially decreased p53 (Figure 2-12B). *mdmX*$^{-/-}$;*p53*$^{KI/-}$;*EμMyc* tumors from tamoxifen-treated recipients also expressed high $p19^{ARF}$ levels but had yet lower levels of p53 protein even than their *mdmX*$^{+/+}$ counterparts (Figure 2-12B). Southern blot analysis revealed that the loss of p53 expression is due to wholesale deletion of the *p53*^{KI} locus (Figure 2-12C). Hence, even though p53 restoration therapy in the absence of MdmX conferred a significant extension of survival in lymphoma-bearing mice, any therapeutic benefit is still limited by the emergence of resistant clones in which the restored p53 pathway has been incapacitated.

FIGURE LEGENDS

Figure 1. p53 is spontaneously active in tissues of *p53$^{KI/-}$;mdmX$^{-/-}$* mice

(A) RNA was isolated from organs of mice treated with either vehicle (oil) or tamoxifen for 6 hours and *cdkn1a* and *puma* gene expression quantified by Taqman analysis. Fold induction (expression in tamoxifen-treated tissues over vehicle-treated tissues) is plotted. Fold inductions that were statistically significant are marked with an asterisk. Error bars show SEM of triplicates.

(B) A single bolus of either vehicle or tamoxifen was administered to mice of the indicated genotypes and organs collected 6 hours later. Apoptosis was detected in tissue sections by TUNEL staining.

Figure 2. Apoptosis was induced after p53 restoration in the subventricular zone (SVZ) of *mdmX$^{-/-}$;p53$^{KI/-}$* mice but not in the cerebellum.

Mice of the indicated genotypes were treated with either vehicle (V) or tamoxifen (T) and tissues collected 6 hours later for immunohistochemical analysis and RNA extraction. Representative TUNEL stainings are shown (arrowheads mark positive cells), together with Taqman analysis of *cdk1na* expression in the cerebellum, which demonstrates p53 had become active. Error bars show SEM of triplicates.

Figure 3. Transient p53 restoration in the absence of MdmX is well tolerated

(A) Kaplan-Meier curve showing survival of mice of the indicated genotypes given daily injections of vehicle or tamoxifen for one week. Controls are: *p53*$^{KI/-}$ mice treated with vehicle (n=8); *p53*$^{KI/-}$ treated with tamoxifen (n=8); *mdm2*$^{-/-}$*;p53*$^{KI/-}$ mice treated with vehicle (n=6); *mdmX*$^{-/-}$*;p53*$^{KI/-}$ mice treated with vehicle (n=13); *mdmX*$^{-/-}$*;p53*$^{-/-}$ mice treated with tamoxifen (n=4).

(B) Mice of the indicated genotypes were treated daily with either vehicle or tamoxifen for 7 days. Left panels show H&E staining of bone marrow, spleen and thymus. Right panels show BrdU staining of the same organs (BrdU was administered 2 hours prior to sacrifice).

(C) H&E, TUNEL and BrdU staining of sections of small intestine from mice treated as in (B).

Figure 4. Small intestine is extremely sensitive to p53 restoration in the absence of Mdm2.

Hematoxilin and eosin staining on small intestine sections from *mdm2*$^{+/+}$*;p53*$^{KI/-}$ and *mdm2*$^{-/-}$*;p53*$^{KI/-}$ mice treated with either vehicle or tamoxifen for 5 days (daily injections), as indicated.

Figure 5. Permanent p53 restoration is lethal in the absence of MdmX

(A) Kaplan-Meier curve showing survival of mice of the indicated genotypes given continuous daily injections of vehicle or tamoxifen. Controls are:

mdmX$^{+/+}$;*p53*$^{KI/-}$ mice treated with tamoxifen (n=13); *mdmX*$^{-/-}$;*p53*$^{KI/-}$ mice treated with vehicle (n=9); *mdmX*$^{-/-}$;*p53*$^{-/-}$ mice treated with tamoxifen (n=6).

(B) H&E staining of organs harvested from *mdmX*$^{+/+}$;*p53*$^{KI/-}$ and *mdmX*$^{-/-}$;*p53*$^{KI/-}$ mice treated continuously with daily tamoxifen for 26 days.

(C) H&E, TUNEL and Ki67 staining of small intestine harvested from *mdmX*$^{+/+}$;*p53*$^{KI/-}$ and *mdmX*$^{-/-}$;*p53*$^{KI/-}$ mice treated continuously with daily tamoxifen for 26 days.

Figure 6. Long term p53 restoration causes anemia in *mdmX*$^{-/-}$;*p53*$^{KI/-}$ mice.

mdmX$^{-/-}$;*p53*$^{KI/-}$ mice treated with tamoxifen for 26 days are severely anemic. Controls are *mdmX*$^{-/-}$;*p53*$^{KI/-}$ mice treated with vehicle and *mdmX*$^{+/+}$;*p53*$^{KI/-}$ mice treated with tamoxifen for 26 days. Error bars show SEM of triplicates.

Figure 7. The pathological effects of transient p53 restoration in the absence of MdmX are reversible

(A) Mice of the indicated genotypes were treated daily with tamoxifen for 7 days and allowed to recover for 7 further days. Left panels show BrdU staining of sections of bone marrow, spleen and thymus (BrdU was administered 2 hours prior to sacrifice). Right panels show H&E staining of the same organs.

(B) H&E, TUNEL and BrdU staining of small intestine sections from mice treated as in (A).

Figure 8. p53 restoration in the absence of Mdm2 acutely depletes HSCs but not in the absence of MdmX

(A) Whole bone marrow was collected from mice of the indicated genotypes after either a short p53 restoration (1 day tamoxifen) or a long p53 restoration (7 days for *p53$^{KI/-}$* and *mdmX$^{-/-}$;p53$^{KI/-}$* mice and only 5 days for *mdm2$^{-/-}$;p53$^{KI/-}$* mice, because of lethality). Total cell counts (excluding red blood cells) are presented.

(B-D) Quantitation of hematopoietic stem cells (HSCs), myeloid cells and mature B-lymphocytes from the same mice as in (A). Insufficient cells were recovered from 5-day treated *mdm2$^{-/-}$;p53$^{KI/-}$* mice for meaningful analysis.

Figure 9. p53 restoration is acutely lethal to mature cells in spleen in the absence of Mdm2, but not in the absence of MdmX.

Spleens were collected from mice of the indicated genotypes after either a short p53 restoration (1 day tamoxifen) or a long p53 restoration (7 days for *p53$^{KI/-}$* and *p53$^{KI/-}$;MdmX$^{-/-}$* mice, however, because of lethality, *p53$^{KI/-}$;Mdm2$^{-/-}$* mice were treated only for 5 days). Total cell count is shown, as well as cell counts for mature myeloid, B and T cells. Not enough cells were recovered from 5-day treated *p53$^{KI/-}$;Mdm2$^{-/-}$* mice for significant analysis of mature cells.

Figure 10. Mdm2 is functional and contributes to p53 downregulation in the absence of MdmX

(A) *mdmX*$^{+/+}$*;p53*$^{KI/-}$ and *mdmX*$^{-/-}$*;p53*$^{KI/-}$ mouse embryonic fibroblasts (MEFs) were treated with either 4-OHT or 4-OHT plus 10 μM Nutlin-3a for the indicated times. Immunoblotting was used to estimate levels of p53 and p21^{cip1} at each time point.

(B) Mice of the indicated genotypes were treated with either vehicle (V) or tamoxifen (T) for one day. The levels of p53 in the livers of these mice are presented (immunoblot, each lane is a separate mouse) together with the relative induction of p53 target genes *cdkn1a* and *mdm2* (by Taqman; *gus* is the control gene). Error bars show SEM of triplicates.

Figure 11. Restoration of p53 in the absence of MdmX extends overall survival in lymphoma-bearing mice

mdmX$^{+/+}$*;p53*$^{KI/-}$*;EμMyc* and *mdmX*$^{-/-}$*;p53*$^{KI/-}$*;EμMyc* tumors (graph legend indicates *mdmX* genotype only) were transplanted into wild type recipients. 10 days after transplant, recipient mice were treated with either vehicle or tamoxifen for 1 week. Their survival is plotted as a Kaplan-Meier curve.

Figure 12. p53 restoration in the absence of MdmX does not prevent emergence of resistant clones that deleted p53 in *EμMyc* tumors.

(A) *mdmX*$^{+/+}$*;p53*$^{KI/-}$*;EμMyc* and *mdmX*$^{-/-}$*;p53*$^{KI/-}$*;EμMyc* transplanted tumors isolated from recipient-mice previously treated with either vehicle (designated as Post-veh) or tamoxifen (designated as Post-Tam) *in vivo* were cultured in the presence or absence of 4-OHT. *In vitro* growth of cells derived from representative tumors is presented.

(B) Immunoblot analysis of p53 and p19^{ARF} levels in transplanted tumors isolated from recipient-mice treated with vehicle (designated as Post-veh) or tamoxifen (designated as Post-Tam). Each lane represents an individual tumor.

(C) Southern blot analysis of DNA isolated from the same tumors as in (B). The p53 probe detects a 5.9 kb band from the *p53*^{KI} locus, a 5.0 kb band from the wild type p53 locus (from the host tissue) and a 3.0 kb band from the p53 knockout locus.

Figure 2-1

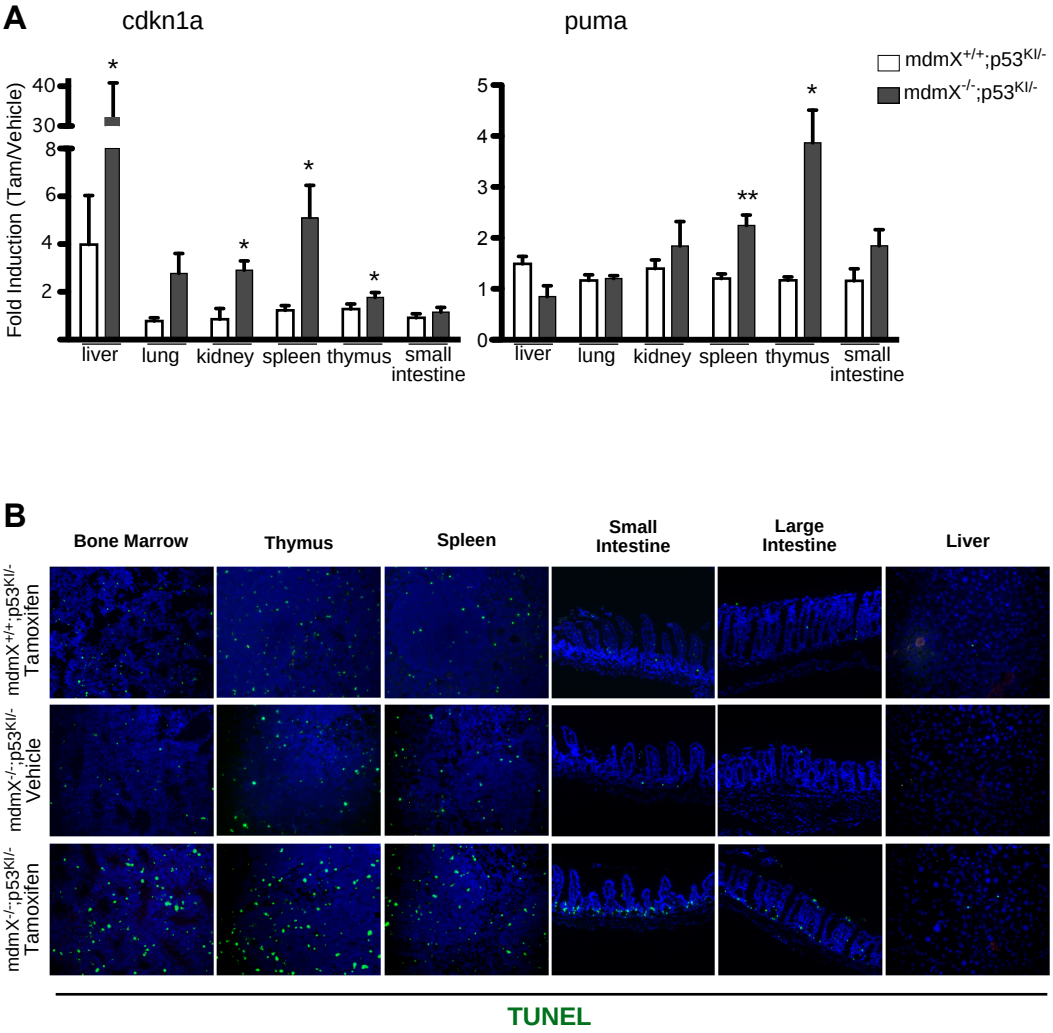
A
cdkn1a
puma
mdmX+/+;p53KI/-
mdmX-/-;p53KI/-
Fold Induction (Tam/Vehicle)
liver
lung
kidney
spleen
thymus
small intestine
B
Bone Marrow
Thymus
Spleen
Small Intestine
Large Intestine
Liver
mdmX+/+;p53KI/- Tamoxifen
mdmX-/-;p53KI/- Vehicle
mdmX-/-;p53KI/- Tamoxifen
TUNEL

Figure 2-2

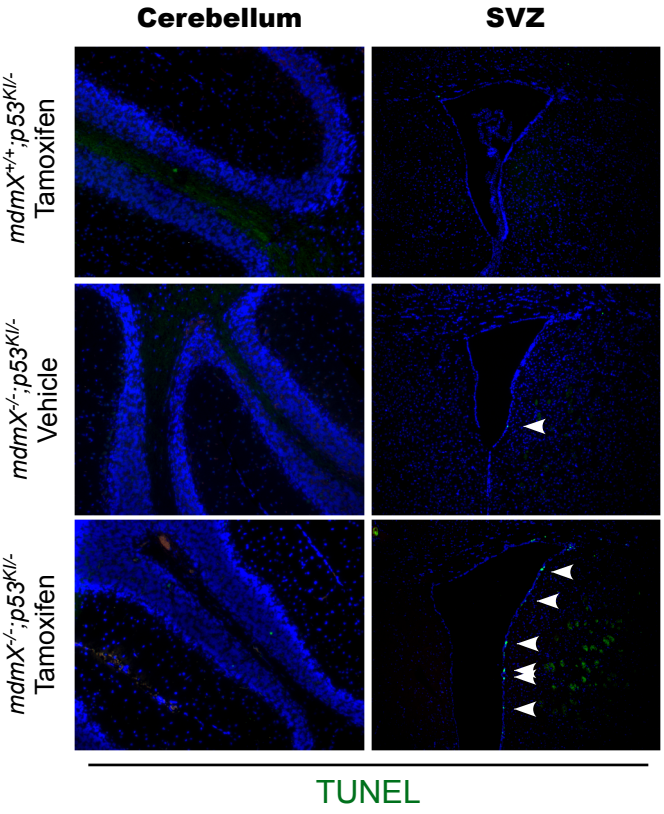
Cerebellum
SVZ
mdmX+/+;p53Kl/- Tamoxifen
mdmX-/-;p53Kl/- Vehicle
mdmX-/-;p53Kl/- Tamoxifen
TUNEL

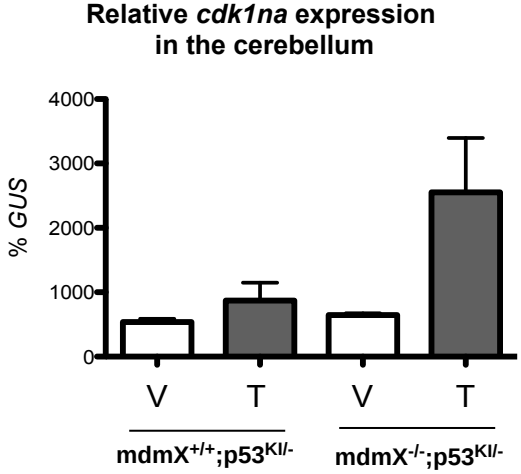
Relative cdk1na expression in the cerebellum
% GUS
4000
3000
2000
1000
0
V
T
V
T
mdmX+/+;p53Kl/-
mdmX-/-;p53Kl/-

Figure 2-3

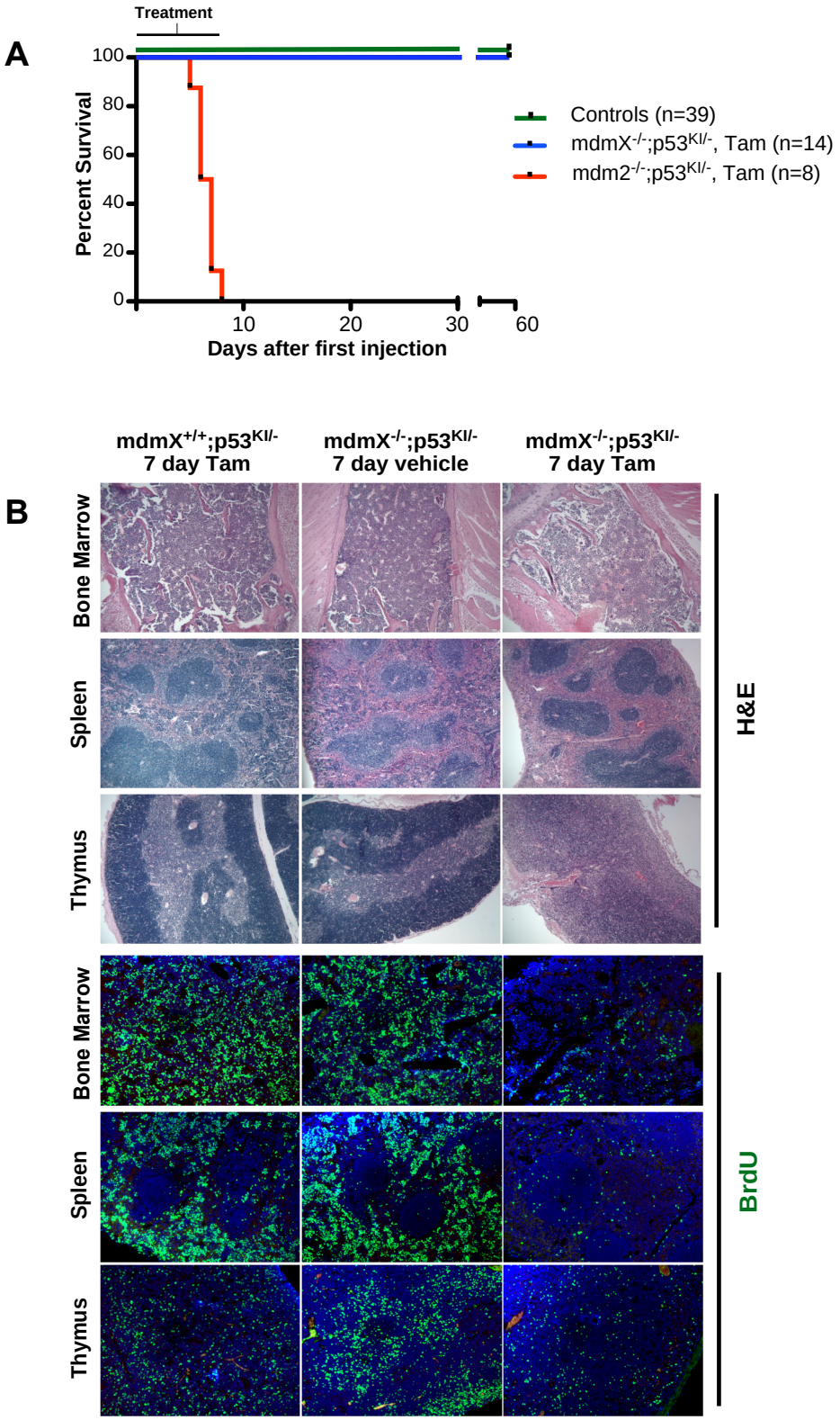
A
Treatment
100
80
60
40
20
0
Percent Survival
10
20
30
60
Days after first injection
Controls (n=39)
mdmX-/-;p53KI/-, Tam (n=14)
mdm2-/-;p53KI/-, Tam (n=8)
B
mdmX+/+;p53KI/-
7 day Tam
mdmX-/-;p53KI/-
7 day vehicle
mdmX-/-;p53KI/-
7 day Tam
Bone Marrow
Spleen
Thymus
H&E
Bone Marrow
Spleen
Thymus
BrdU

Figure 2-3 (cont.)

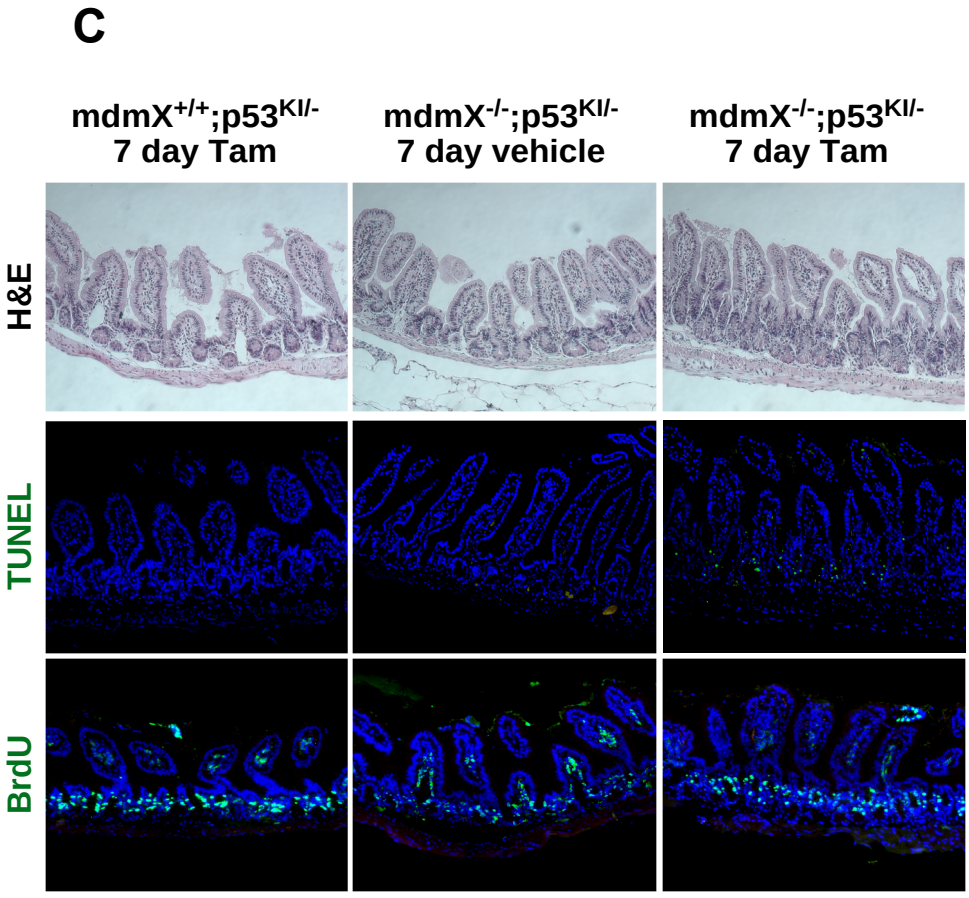

Figure 2-4


mdm2+/+;p53KI/-
5 days tamoxifen
mdm2-/-;p53KI/-
5 days vehicle
mdm2-/-;p53KI/-
5 days tamoxifen
H&E

Figure 2-5

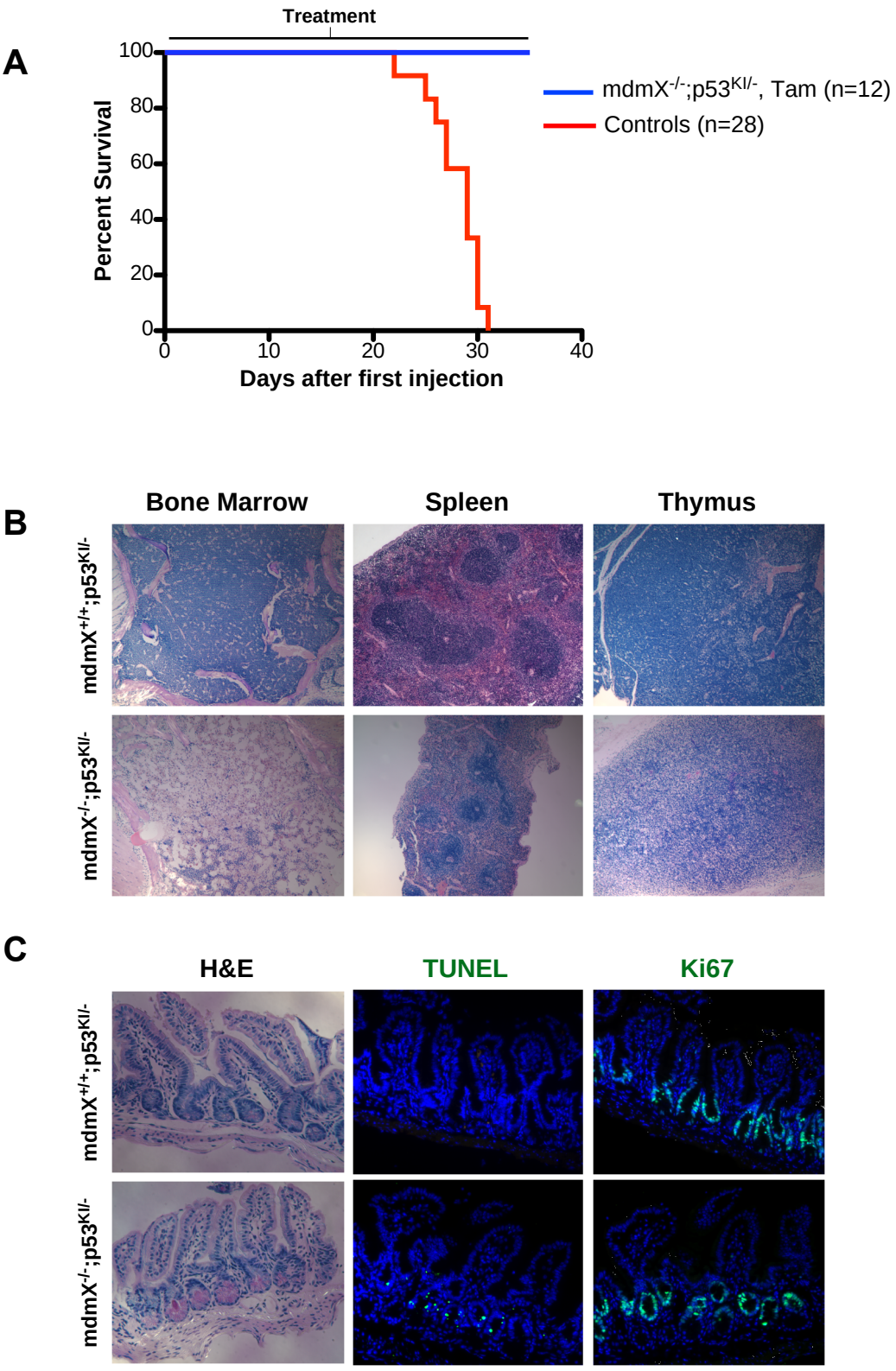
A
Treatment
100
80
60
40
20
0
Percent Survival
0
10
20
30
40
Days after first injection
mdmX-/-;p53KI/-, Tam (n=12)
Controls (n=28)
B
Bone Marrow
Spleen
Thymus
mdmX+/+;p53KI/-
mdmX-/-;p53KI/-
C
H&E
TUNEL
Ki67
mdmX+/+;p53KI/-
mdmX-/-;p53KI/-

Figure 2-6

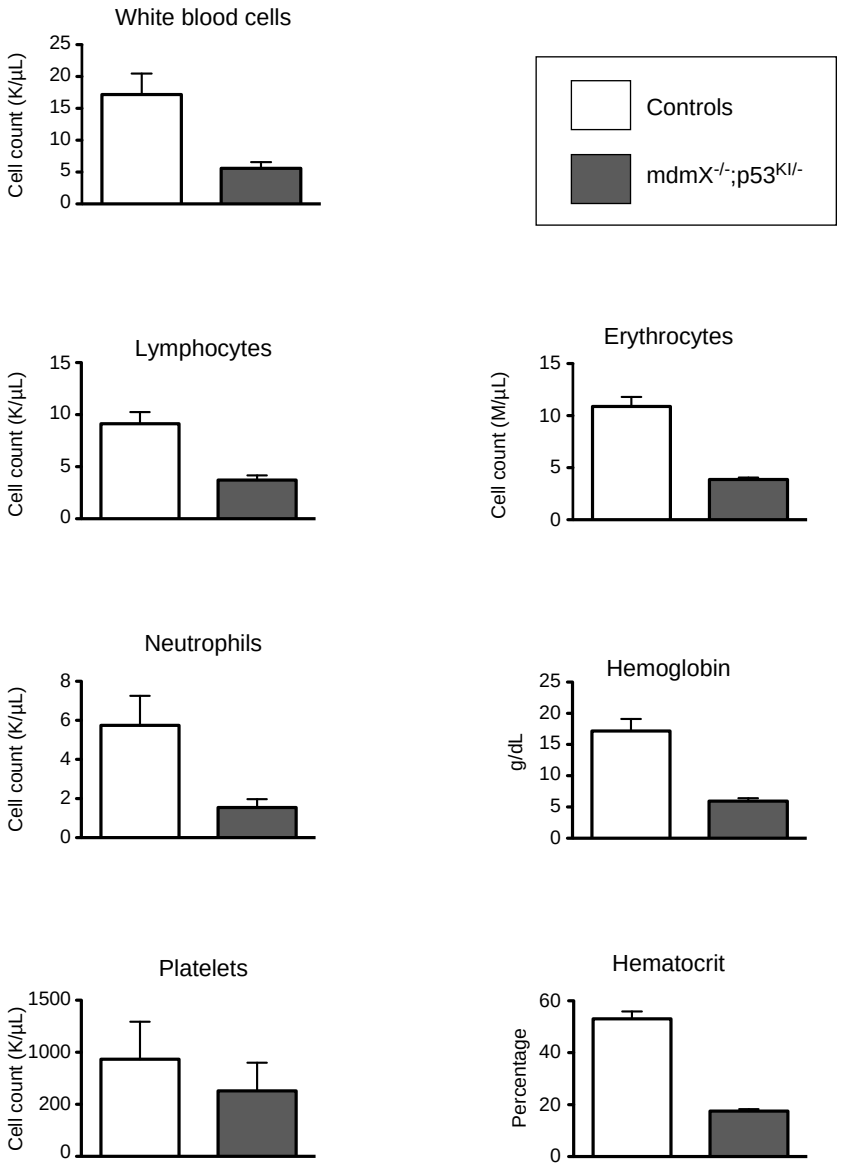
White blood cells
Cell count (K/µL)
25
20
15
10
5
0
Controls
mdmX-/-;p53KI/-
Lymphocytes
Cell count (K/µL)
15
10
5
0
Erythrocytes
Cell count (M/µL)
15
10
5
0
Neutrophils
Cell count (K/µL)
8
6
4
2
0
Hemoglobin
g/dL
25
20
15
10
5
0
Platelets
Cell count (K/µL)
1500
1000
200
0
Hematocrit
Percentage
60
40
20
0

Figure 2-7

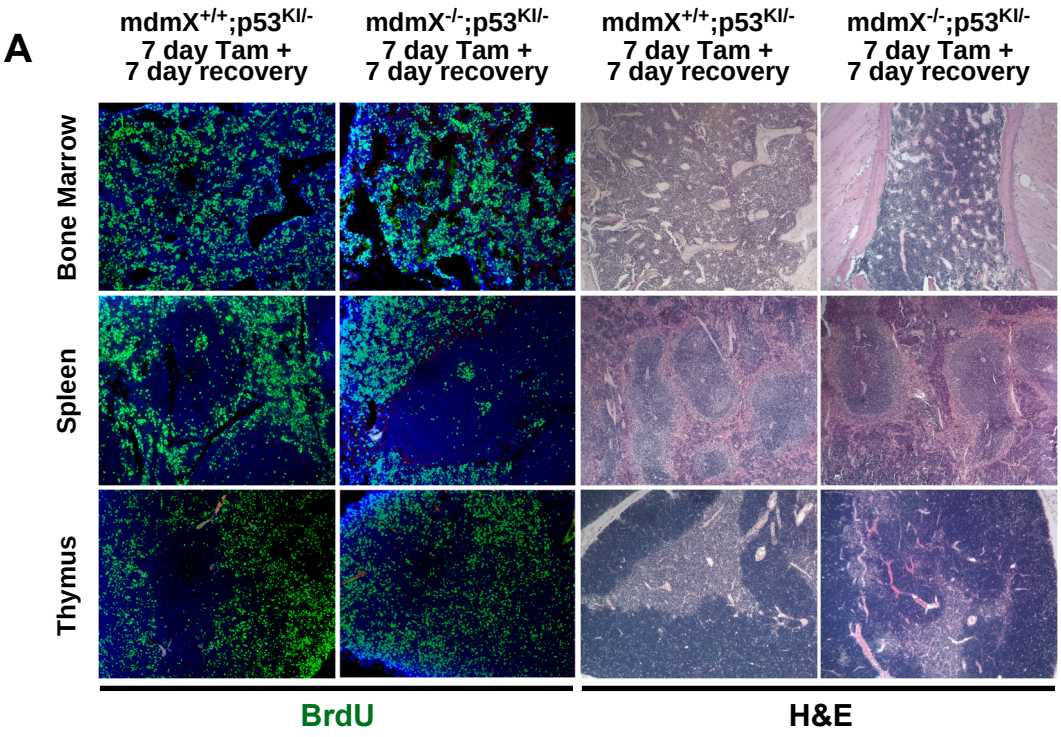
A
mdmX+/+;p53KI/- 7 day Tam + 7 day recovery
mdmX-/-;p53KI/- 7 day Tam + 7 day recovery
mdmX+/+;p53KI/- 7 day Tam + 7 day recovery
mdmX-/-;p53KI/- 7 day Tam + 7 day recovery
Bone Marrow
Spleen
Thymus
BrdU
H&E
B
mdmX+/+;p53KI/- 7 day Tam + 7 day recovery
mdmX-/-;p53KI/- 7 day Tam + 7 day recovery
H&E
TUNEL
BrdU

Figure 2-8

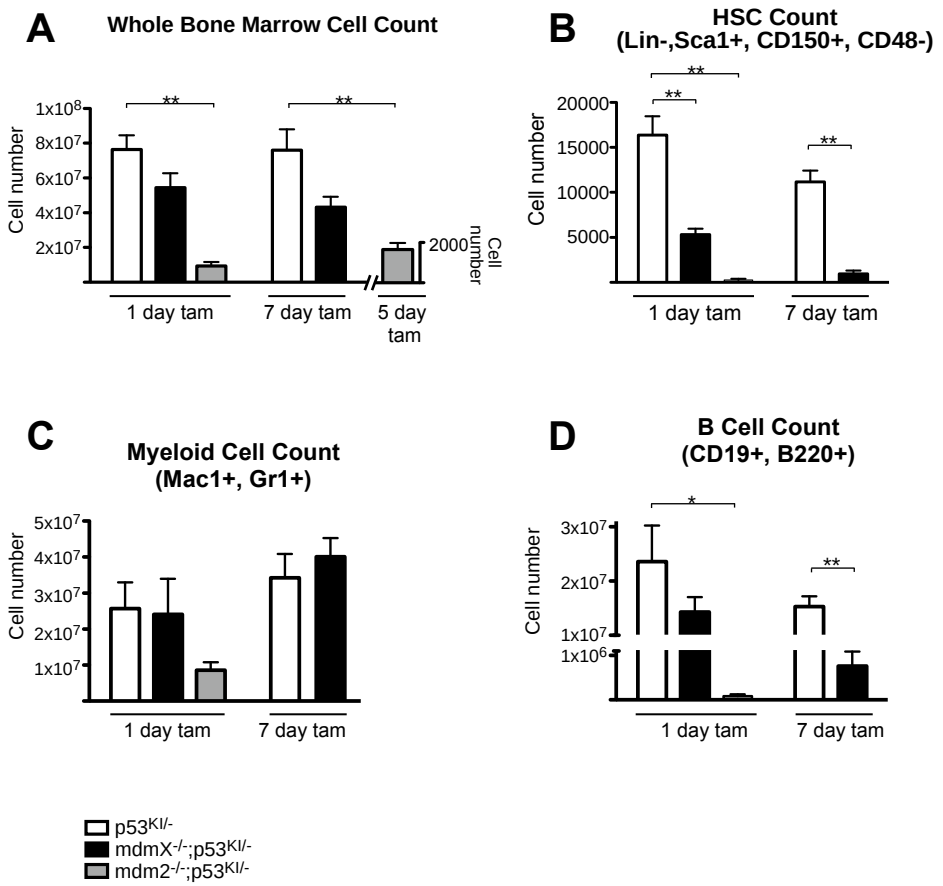
A
Whole Bone Marrow Cell Count
Cell number
1x10^8
8x10^7
6x10^7
4x10^7
2x10^7
2000
Cell number
**
**
1 day tam
7 day tam
5 day tam
B
HSC Count
(Lin-,Sca1+, CD150+, CD48-)
Cell number
20000
15000
10000
5000
**
**
**
1 day tam
7 day tam
C
Myeloid Cell Count
(Mac1+, Gr1+)
Cell number
5x10^7
4x10^7
3x10^7
2x10^7
1x10^7
1 day tam
7 day tam
D
B Cell Count
(CD19+, B220+)
Cell number
3x10^7
2x10^7
1x10^7
1x10^6
*
**
1 day tam
7 day tam
p53KI/-
mdmX-/-;p53KI/-
mdm2-/-;p53KI/-

Figure 2-9

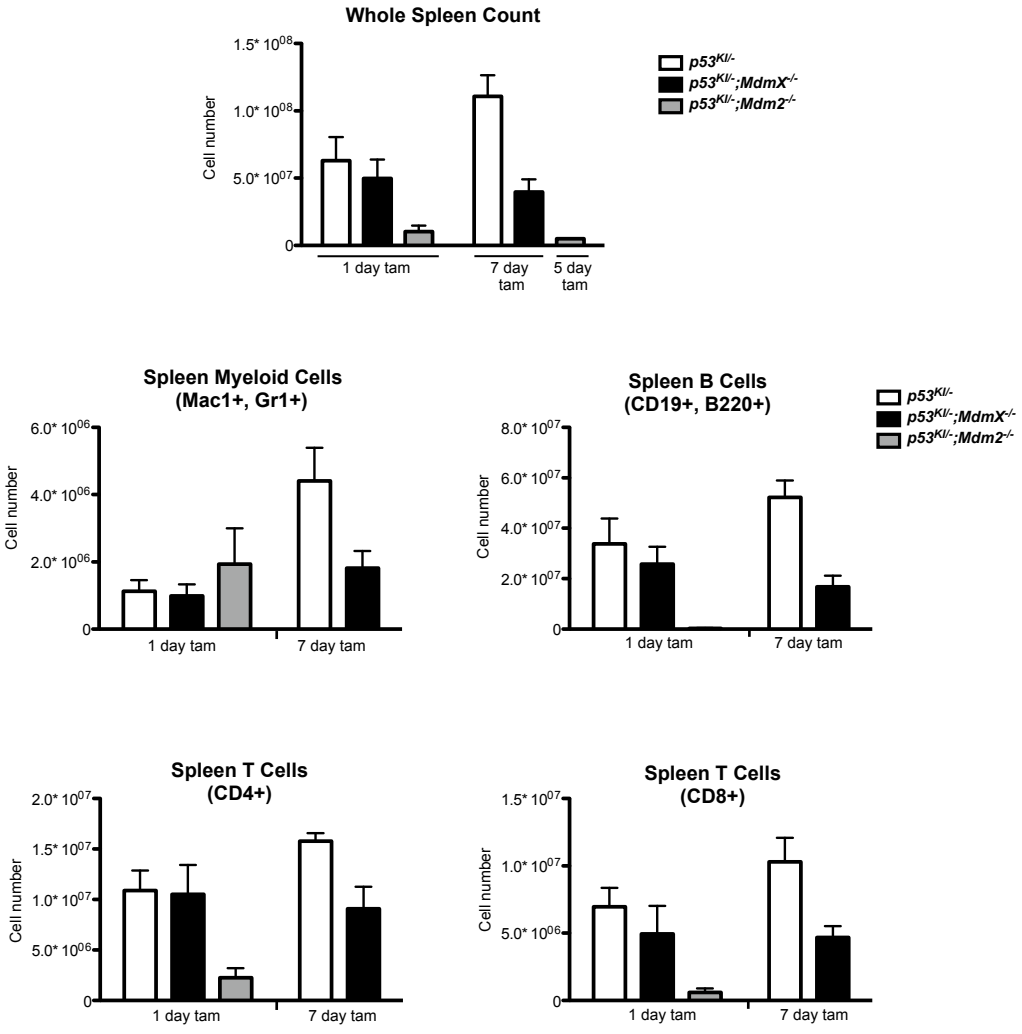
Whole Spleen Count
Cell number
1.5* 10^08
1.0* 10^08
5.0* 10^07
0
1 day tam
7 day tam
5 day tam
p53KI/-
p53KI/-;MdmX-/-
p53KI/-;Mdm2-/-
Spleen Myeloid Cells (Mac1+, Gr1+)
6.0* 10^06
4.0* 10^06
2.0* 10^06
1 day tam
7 day tam
Spleen B Cells (CD19+, B220+)
8.0* 10^07
6.0* 10^07
4.0* 10^07
2.0* 10^07
Spleen T Cells (CD4+)
2.0* 10^07
1.5* 10^07
1.0* 10^07
5.0* 10^06
Spleen T Cells (CD8+)
1.5* 10^07
1.0* 10^07
5.0* 10^06

Figure 2-10

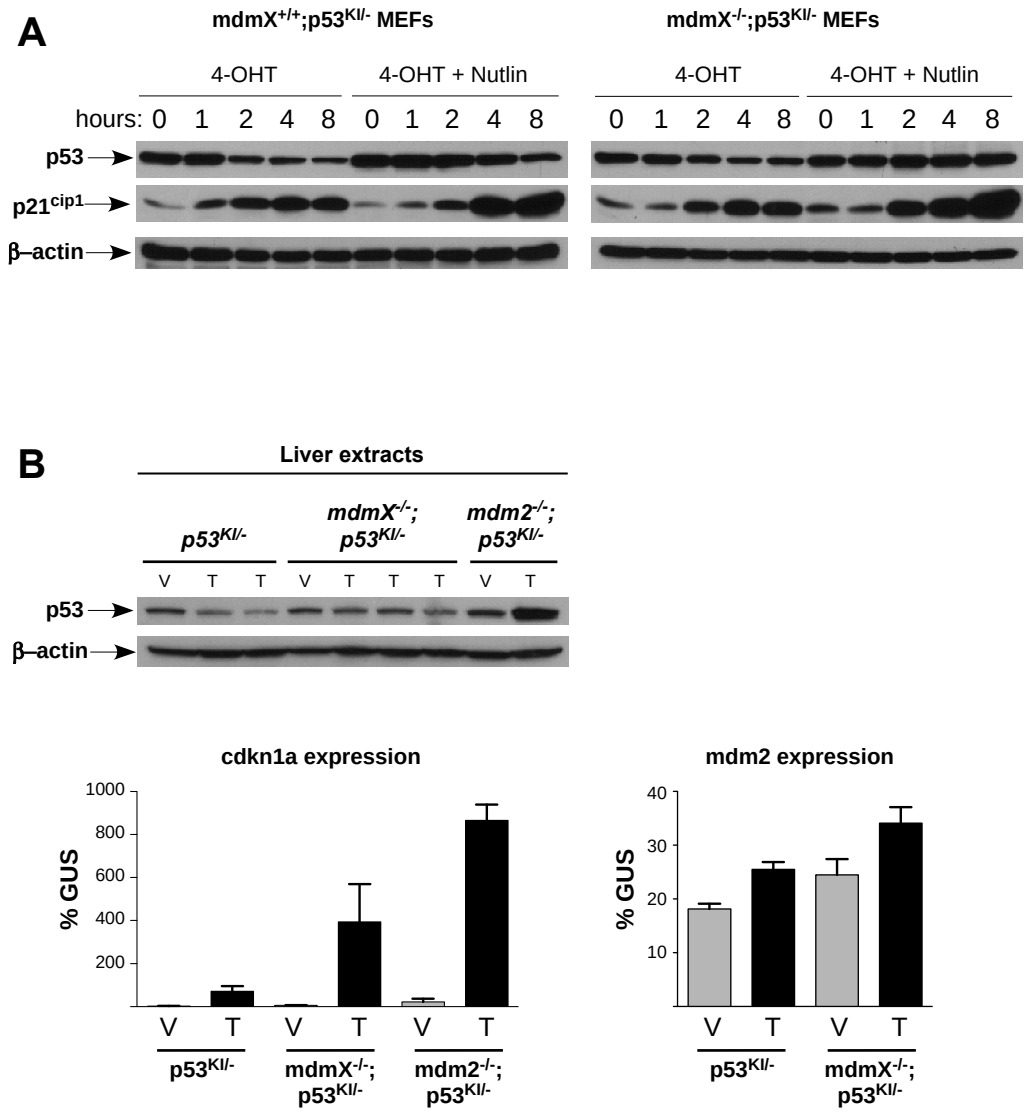
A
mdmX+/+;p53KI/- MEFs
mdmX-/-;p53KI/- MEFs
4-OHT
4-OHT + Nutlin
hours: 0 1 2 4 8 0 1 2 4 8
0 1 2 4 8 0 1 2 4 8
p53
p21cip1
β–actin
B
Liver extracts
p53KI/-
mdmX-/-; p53KI/-
mdm2-/-; p53KI/-
V T T V T T T V T
p53
β–actin
cdkn1a expression
% GUS
1000
800
600
400
200
V T V T V T
p53KI/-
mdmX-/-; p53KI/-
mdm2-/-; p53KI/-
mdm2 expression
% GUS
40
30
20
10
V T V T
p53KI/-
mdmX-/-; p53KI/-

Figure 2-11

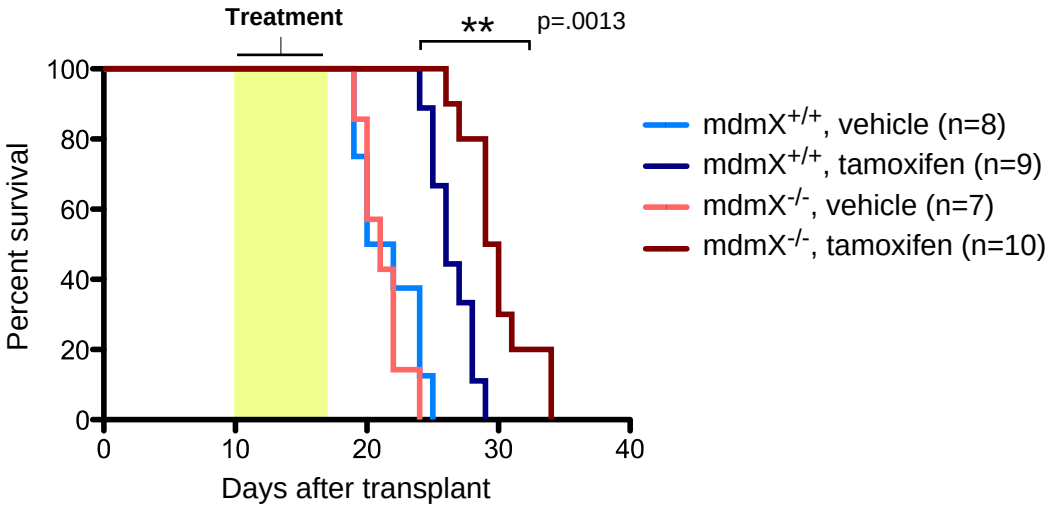
Treatment
**
p=.0013
100
80
60
40
20
0
Percent survival
0
10
20
30
40
Days after transplant
mdmX+/+, vehicle (n=8)
mdmX+/+, tamoxifen (n=9)
mdmX-/-, vehicle (n=7)
mdmX-/-, tamoxifen (n=10)

Figure 2-12

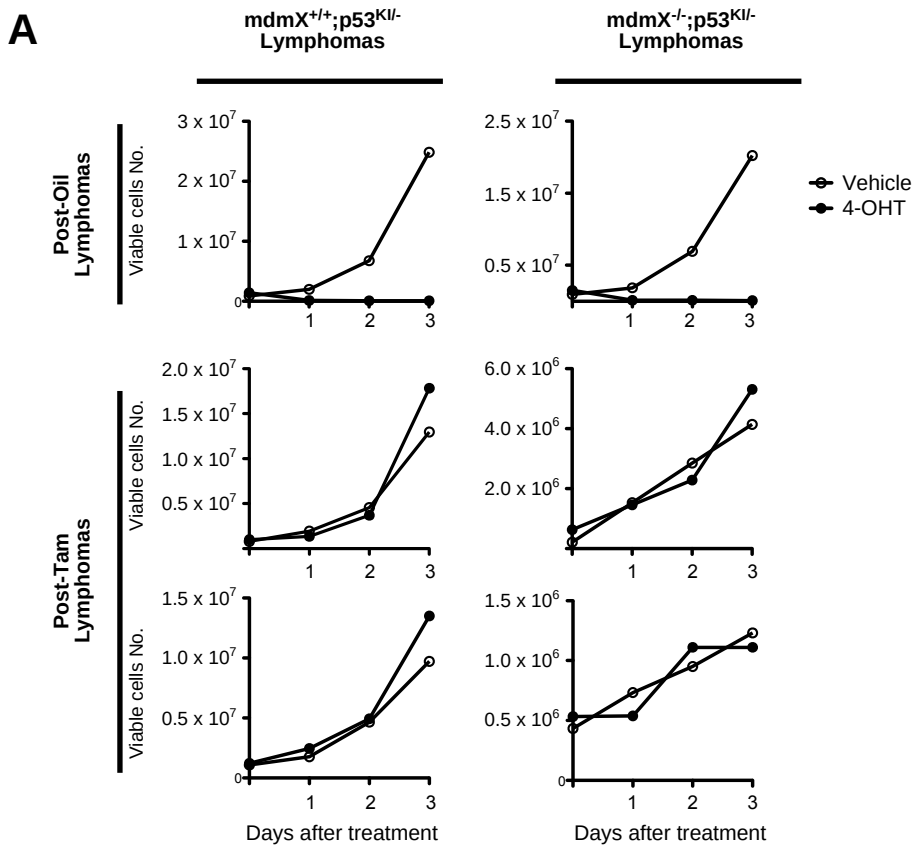
A
mdmX+/+;p53KI/- Lymphomas
mdmX-/-;p53KI/- Lymphomas
Post-Oil Lymphomas
Post-Tam Lymphomas
Viable cells No.
Vehicle
4-OHT
Days after treatment
Days after treatment

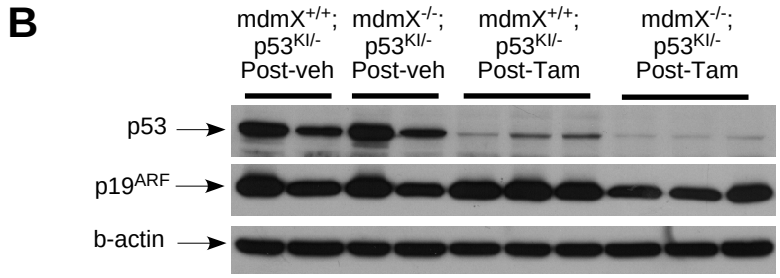
B
mdmX+/+; p53KI/- Post-veh
mdmX-/-; p53KI/- Post-veh
mdmX+/+; p53KI/- Post-Tam
mdmX-/-; p53KI/- Post-Tam
p53
p19ARF
b-actin

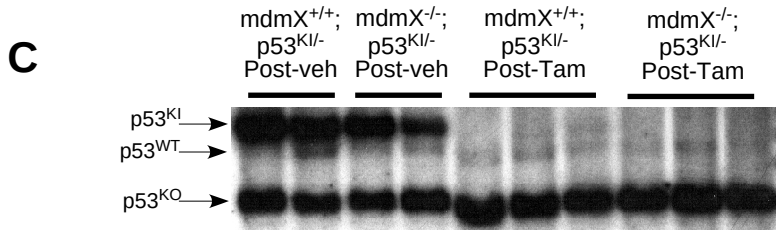
C
mdmX+/+; p53KI/- Post-veh
mdmX-/-; p53KI/- Post-veh
mdmX+/+; p53KI/- Post-Tam
mdmX-/-; p53KI/- Post-Tam
p53KI
p53WT
p53KO

CHAPTER 3

Tet-repressor targeting E2F3

Generation of *e2f3*^{tre} mice.

To target the endogenous *e2f3* locus for tTS-mediated repression, we inserted the TRE DNA fragment into the *e2f3a* promoter. We hypothesized that having a binding site in the promoter would increase the chances of achieving efficient repression. The *e2f3a* promoter contains numerous binding sites for transcription factors, including E2F and E-box sites (Adams et al. 2000). After careful analysis of the promoter, a KpnI site that did not interfere with transcription binding sequences was identified just upstream of the transcription start site. A targeting vector was constructed in which the TRE sequence, together with a floxed Neo cassette, was introduced in the aforementioned KpnI site (Figure 3-1A). In addition, silent mutations were introduced into both exons 1a and 1b, so that mRNA derived from the TRE-targeted allele could be distinguished from mRNA derived from the wild type allele. Embryonic stem cells were electroporated with the finished targeting vector. Correctly recombined embryonic stem cell clones (Figure 3-1B) were transiently transfected with a vector that expressed Cre to excise the Neo cassette. A clone that completely excised the Neo cassette was microinjected into embryos to generate chimeras, which eventually produced germline *e2f3*$^{tre/+}$ mice.

At the time of cloning, *e2f3a* and *e2f3b* single knockout mice had not been generated. For this reason, a second targeting vector was constructed that would allow generation of *e2f3a* and *e2f3b* single knockout mice (Figure 3-2). These mice would have allowed us to address important unresolved questions about the distinct biology of E2F3a and E2F3b. The TRE sequence was inserted in the

same location as in the previous targeting vector and the same silent mutations were introduced. The Neo cassette, LoxP and FRT sites were introduced as indicated (Figure 3-2). After electroporation, correctly recombined embryonic stem cell clones were transiently transfected with a vector that expressed low levels of the Flp recombinase. Upon screening, one clone was found that had partially recombined its FRT sites, this is, only the Neo was excised, but not exon 1a (Figure 3-2). This clone was microinjected into embryos to generate chimeras, which eventually produced germline *e2f3*$^{treFL/+}$ mice (FL= floxed and flrted allele). In these cells, *e2f3a* knockout mice can be generated by expression of Flp (leaving behind a switchable *e2f3b* gene) and *e2f3b* knockout mice can be generated by expression of Cre (leaving behind a switchable *e2f3a* gene). Unfortunately, soon after germline transmission was obtained, generation of *e2f3a* and *e2f3b* single knockout mice was published by two other groups (Tsai et al. 2008; Danielian et al. 2008). Consequently, *e2f3*$^{treFL/treFL}$ mice became second priority. No further experiments were performed on these mice.

Insertion of TRE does not disrupt normal *e2f3* regulation.

Given the complex regulation of the *e2f3* gene, we wished to determine first whether the insertion of the TRE DNA fragment had any effect on normal E2F3 transcriptional regulation. *e2f3a* is a cell cycle regulated gene, whose expression level is low in quiescent cells but increases as cells enter into S phase. *e2f3b*, on the other hand, is not significantly regulated by cell cycle status and is expressed constitutively in MEFs (Adams et al. 2000). To determine if this regulation still

takes place in the TRE-targeted allele, we generated *e2f3*$^{+/tre}$ MEFs and serum-starved them for 48 hours to synchronize their cell cycle status. Because of silent mutations introduced, distinct Taqman probes can differentiate between mRNA generated from the TRE-targeted allele from mRNA generated from the wild type allele. Using heterozygote MEFs also allowed us to measure both mRNAs in the very same cells, eliminating potentially confounding variability of separate MEF cell lines. After serum addition, the fold induction of TRE-allele derived and wild type allele derived mRNA was identical for both *e2f3a* and *e2f3b* as cells re-entered the cell cycle (Figure 3-3A). Importantly, TRE-allele derived *e2f3a* mRNA exhibited the expected cell-cycle regulated increase at the onset of S phase and TRE-allele derived *e2f3b* mRNA was only mildly affected by cell cycle reentry, similar to wild type derived mRNAs. We conclude that insertion of the TRE sequence did not disrupt normal transcriptional regulation of the *e2f3* gene.

E2F3 is also regulated at the protein level during cell cycle progression. To determine if protein derived from *e2f3*^{tre}alleles exhibited normal regulation we generated *e2f3*$^{tre/tre}$ and wild type littermate MEFs, serum starved them for 48 hours and forced their reentry into cycle by addition of serum. E2F3a protein levels showed similar temporal induction in *e2f3*$^{tre/tre}$ and wild type MEFs, whereas E2F3b showed no change in either (Figure 3-3B), mirroring the transcriptional regulation described above. Hence, E2F3 proteins exhibit normal regulation in *e2f3*$^{tre/tre}$ cells.

The tTS repressor irreversibly represses *e2f3^{tre}* expression when mice develop without doxycycline.

To test whether tTS could repress *e2f3^{tre}* expression, we crossed *e2f3^{tre}* mice to a mouse transgenic line that constitutively expresses the tTS repressor from the β-actin promoter in all tissues (made in Shaun Coughlin's lab, unpublished) to generate *e2f3$^{+/tre}$;β-actin-tTS* mice (*e2f3$^{+/tre}$;tTS* mice, hereafter). These mice were then crossed to generate *e2f3$^{tre/tre}$;tTS* MEFs. Indeed, no E2F3 was detected in all *e2f3$^{tre/tre}$;tTS* MEF cell lines tested, confirming that tTS had efficiently repressed e2f3 expression in these cells (Figure 3-4A). However, this repression was not relieved upon addition of doxycycline and appeared to be permanent, as even extended exposure to doxycycline failed to de-repress e2f3 expression in *e2f3$^{tre/tre}$;tTS* MEFs *in vitro* (Figure 3-4A). To determine if this was also true *in vivo*, we took *e2f3$^{+/tre}$;tTS* mice that developed in the absence of doxycycline and exposed them to doxycycline (1 mg/ml, in their drinking water) for two weeks. No *e2f3a* or *e2f3b* mRNA derived from the *e2f3^{tre}* allele was detected in liver, spleen or thymus of *e2f3$^{+/tre}$;tTS* mice that developed in the absence of doxycycline (Figure 3-4B) (the *e2f3b* Taqman probe gives a small background signal, which is shown). Similarly, no *e2f3a* or *e2f3b* mRNA derived from the *e2f3^{tre}* allele was detected in liver, spleen or thymus of these *e2f3$^{+/tre}$;tTS* mice even after two weeks of exposure to doxycycline. Hence, *e2f3* is efficiently repressed by tTS *in vivo*, however, this repression is irreversible when mice develop in the absence of doxycycline. Indeed, no *e2f3$^{tre/tre}$;tTS* mice

were ever born from breeders kept off doxycycline, consistent with total loss of E2F3 and the known embryonic lethality associated with it.

tTS efficiently represses the *e2f3*^{tre} allele and this repression is reversible when mice develop in the presence of doxycycline.

To determine if the tTS molecular switch might still function when mice develop in the presence of doxycycline, we bred *e2f3*$^{+/tre}$*;tTS* mice in the presence of doxycycline to generate *e2f3*$^{tre/tre}$*;tTS* MEFs. Remarkably, both *e2f3a* and *e2f3b* mRNA were readily detectable in these *e2f3*$^{tre/tre}$*;tTS* MEFs (Figure 3-5A), confirming that tTS was inactive in the presence of doxycycline and did not repress *e2f3* expression. More importantly, tTS efficiently and completely repressed both *e2f3a* and *e2f3b* as doxycycline cleared from the cells in the continuing passages (Figure 3-5A). Moreover, off-doxycycline *e2f3*$^{tre/tre}$*;tTS* MEFs that had completely repressed *e2f3* expression quickly regained *e2f3* expression when doxycycline was added again to culture media (Figure 3-5A). As expected, presence or absence of doxycycline makes has no impact on E2F3 expression in non-tTS transgenic *e2f3*$^{tre/tre}$ MEFs (Figure 3-5B). Western blot analysis of E2F3 levels in *e2f3*$^{tre/tre}$*;tTS* MEFs from embryos that developed in the presence of doxycycline essentially mirrored the mRNA dynamics: E2F3 proteins disappear as doxycycline is cleared in the continuing passages (Figure 3-5C). Of note, E2F3a levels drop in MEFs in later passages as they loose proliferating potential (Figure 3-5B, passage 7). Accordingly, when *e2f3* expression is restored in later passages, E2F3a is restored at low levels as well (Figure 3-5C, passage 7),

consistent with the notion that the relieved tTS repression does not overexpress the targeted gene, but only allows normal regulation and normal levels to be realized.

To test whether the tTS switch was functional *in vivo*, we took *e2f3*$^{tre/tre}$*;tTS* mice and removed them from doxycycline at weaning to allow repression to take place. Initial experiments showed only mild repression of *e2f3*, even after 10 weeks off doxycycline (data not shown). Two specific steps were taken to optimize repression: first, we lowered the concentration of doxycycline to 100 μg/ml (in drinking water) and second, *e2f3*$^{tre/tre}$*;tTS* mice were bred to generate *e2f3*$^{tre/tre}$*;tTS/tTS* mice, in order to have higher levels of tTS repressor. Thus, *e2f3*$^{tre/tre}$*;tTS/tTS* mice that developed in the presence of doxycycline (100 μg/ml, in drinking water) were removed from doxycycline at weaning (3 weeks of age) to allow repression to take place and *e2f3* mRNA levels were measured in selected proliferating and non-proliferating tissues over 6 consecutive weeks. tTS efficiently repressed *e2f3* expression *in vivo*, albeit with different dynamics in different tissues. Spleen and thymus showed reduction of *e2f3a* mRNA by 3-4 weeks, but was only consistently repressed by 6 weeks after weaning (Figure 3-6A). The small intestine showed robust *e2f3a* repression by 4 weeks off doxycycline and no *e2f3a* mRNA was detected at all after that (Figure 3-6A). Heart and liver are non-proliferating tissues and therefore have low levels of *e2f3a* to begin with. These tissues showed complete repression of *e2f3a* by 3 weeks off doxycycline (Figure 3-6A). *e2f3b*, on the other hand, showed less

variability in its repression dynamics. Small intestine, heart and liver showed robust *e2f3b* repression by 3-4 weeks, unlike spleen and thymus. Importantly, all tested tissues showed virtually complete *e2f3b* repression by 6 weeks off doxycycline (Figure 3-6B). In conclusion, tTS can function as a molecular switch *in vivo* and efficiently represses $e2f3^{tre}$ in tissues of $e2f3^{tre/tre}$*;tTS/tTS* mice.

_e2f3_ repression recapitulates E2F3-knockout phenotypes _in vitro_, but not _in vivo._

Loss of E2F3 has previously been reported to impair the proliferation of MEFs (Humbert et al. 2000). To investigated whether repression of E2F3 would recapitulate the E2F3-knockout phenotype we first took $e2f3^{tre/tre}$*;tTS* MEFs from embryos that developed in the presence of doxycycline and grew them *in vitro* with or without doxycycline. Consistent with E2F3-knockout MEFs, repression of E2F3 had a significant impact on cellular proliferation, as $e2f3^{tre/tre}$*;tTS* MEFs kept without doxycycline grew much slower than MEFs exposed to doxycycline (Figure 3-7). Interestingly, restoration of E2F3 also restored normal proliferation rates, demonstrating the critical role that E2F3 plays as a driver of cellular proliferation in MEFs (Figure 3-7).

E2F3 deficiency was previously reported to be mostly embryonic lethal, with the only a few surviving mice dying as juveniles from heart failure (Humbert et al. 2000; Cloud et al. 2002; King et al. 2008). In our genetic background, however, repression of E2F3 is fully embryonic lethal, as no $e2f3^{tre/tre}$*;tTS* mice are ever born unless doxycycline is provided during development, further

supporting E2F3 as an essential gene for development. To test whether E2F3 was also essential for adult mouse viability, we took *e2f3*$^{tre/tre}$*;tTS/tTS* mice and removed them from doxycycline at weaning and monitored their health and viability over time. As described above (Figure 3-6), both *e2f3a* and *e2f3b* are efficiently repressed by tTS by 6 weeks after weaning. Hence, these mice develop with E2F3 and become effectively E2F3-null at the onset of adulthood. In an ongoing experiment, three separate cohorts of *e2f3*$^{tre/tre}$*;tTS/tTS* mice had been kept off doxycycline for 23, 29 and 37 weeks at the time this thesis was written (Figure 3-8), which means these mice have had no E2F3 for 17, 23 and 31 weeks respectively. Importantly, all *e2f3*$^{tre/tre}$*;tTS/tTS* mice kept off doxycycline have survived and are healthy, similarly to control mice kept on doxycycline (Figure 3-8). These data strongly indicate that E2F3 is not essential for adult homeostasis and viability. This stands in stark contrast to the E3F3-knockout phenotype. We have therefore uncovered, for the first time, a gene known to be required for embryonic development, but is nonetheless dispensable for adult viability.

Repression of *e2f3* is not therapeutically beneficial in a mouse model of lymphoma.

Given the numerous reports implicating E2F3 in cancer, we whished to determine whether *e2f3* repression would be therapeutically beneficial in established tumors. To test this, we crossed *e2f3*$^{tre/tre}$*;tTS* mice to lymphoma-prone *Eμ-Myc* transgenic mice (Adams et al. 1985). *e2f3*$^{tre/tre}$*;tTS;EμMyc* mice

were kept on doxycycline until they developed tumors. *e2f3*$^{tre/tre}$*;tTS;Eμ Myc* tumors were then collected and transplanted into wild type recipients that were kept either on or off doxycycline after transplant (Figure 3-9A). All collected tumors retained *e2f3* expression, consistent with the predicted inactivity of tTS in the presence of doxycycline (Figure 3-9B). Importantly, *e2f3* was rapidly and efficiently repressed by one week in tumors transplanted into recipients kept off doxycycline (Figure 3-9C). Interestingly, however, repression of *e2f3* did not confer a survival advantage to mice kept off doxycycline compared to controls (Figure 3-10A).

Eμ Myc lymphomas often select against genes or pathways that negatively impact their progression (Martins et al. 2006). To determine if *e2f3* repression had been selected against (for example by loss of the tTS transgene), we analyzed *e2f3* levels in tumors at sacrifice point. All tested *e2f3*$^{tre/tre}$*;tTS;Eμ Myc* tumors kept off doxycycline had low levels or no *e2f3a* and *e2f3b* compared to doxycycline-exposed controls, confirming that *e2f3* remained repressed throughout the experiment and it had not been selected against in recipients kept off doxycycline (Figure 3-10B). Altogether, our data suggests *e2f3* repression has no therapeutic benefit at least in this mouse model of lymphoma.

Figure 3-1. Cloning strategy to generate *e2f3^{tre}* mice.

A) Schematic representation of the 5' end of the mouse *e2f3* locus, the targeting vector and the *e2f3^{tre}* allele obtained after homologous recombination. Exons 1a, 1b and 2 are shown as black boxes. The Neo cassette, flanked by *loxP* sites (black arrowheads), the tet-responsive element and the diphtheria toxin gene are shown as clear boxes. Asterisks mark exons where silent mutations were introduced so that mRNA from the TRE-targeted allele could be distinguished from wild type mRNA by Taqman.

B) Southern blot showing two recombined clones (BglII digest). Stem cell clones that recombined correctly (by homologous recombination) were transiently transfected with a Cre-expressing vector to eliminate the Neo cassette. A clone that deleted the Neo cassette was microinjected to generate chimeric mice.

Figure 3-2. Cloning strategy to generate *e2f3^{treFL}* mice.

A) Schematic representation (not drawn to scale) of the 5' end of the mouse *e2f3* locus, the targeting vector and the *e2f3^{treFL}* allele obtained after homologous recombination. Exons 1a, 1b and 2 are shown as black boxes. The Neo cassette, the tet-responsive element and the diphtheria toxin gene are shown as clear boxes. *loxP* sites (black arrowheads) and FRT-sites (clear arrowheads) are also indicated. Asterisks mark exons where silent mutations were introduced so that mRNA from the TRE-targeted allele could be

distinguished from wild type mRNA by Taqman. Stem cell clones that recombined correctly (homologous recombination) were transiently transfected with a Flp-expressing vector to eliminate the Neo cassette. A clone that deleted the Neo cassette, but that did not delete exon 1a (partial recombination), was microinjected to generate chimeric mice.

Figure 3-3. Insertion of TRE does not disrupt normal *e2f3* regulation

A) Taqman analysis of e2f3a and e2f3b mRNA expression in $e2f3^{+/tre}$ MEFs. Cells were serum starved for 48 hours. Serum was then added and e2f3 mRNA levels were assessed at the indicated time points (in hours). Fold induction is virtually identical for mRNA coming from either the wild type or TRE-targeted allele.

B) Western blot analysis of E2F3 levels on wild type or $e2f3^{tre/tre}$ MEFs. Cells were serum starved for 48 hours. Serum was then added and E2F3 protein levels were assessed at the indicated time points (in hours). E2F3a levels peaks at 16-20 hours for both wild type and TRE-targeted MEFs. E2F3b levels do not change in either one.

Figure 3-4. *$e2f3^{tre}$* is irreversibly repressed by tTS repressor when mice develop without doxycycline.

A) Western blot analysis of E2F3 levels in four independent *$e2f3^{tre/tre}$* MEF cell lines that were derived from embryos that developed without doxycycline. MEFs were grown in culture with or without doxycycline (for at least two

passages), as indicated. Two lines are transgenic for the tTS repressor (lanes 2-5), while the other two lines are not (lanes 6-9). No E2F3 protein was detected in tTS transgenic cells.

B) Taqman analysis of *e2f3a* and *e2f3b* mRNA levels in liver (li), spleen (sp) and thymus (th) of two adult *e2f3*$^{+tre}$*;tTS* mice. Both mice developed without doxycycline. One was put on doxycycline for two weeks prior to sacrifice, while the other one was kept off doxycycline. No *e2f3* mRNA from the TRE-targeted allele was detected even after exposure to doxycycline.

Figure 3-5. tTS efficiently represses the *e2f3*^{tre} allele and this repression is reversible.

A) Taqman analysis of *e2f3* expression in *e2f3*$^{tre/tre}$*;tTS* MEFs. MEFs were expanded in the presence of doxycycline and were then split into doxy (+) and no doxy media (–) at passage 3. *e2f3* mRNA levels were measured at the end of each passage. After passage 5, half of the "no doxy" MEFs were reversed back into doxycycline containing media (R). n.d.= not detected.

B) Western blot analysis of E2F3 levels in *e2f3*$^{tre/tre}$ MEFs. MEFs were expanded in the presence of doxycycline and were then split into doxy (+) and no doxy media (–) at passage 3. E2F3 levels were measured at the end of each passage. Doxycycline does not affect E2F3 levels in the absence of the tTS repressor.

C) Western blot analysis of E2F3 levels in *e2f3*$^{tre/tre}$*;tTS* MEFs. MEFs were expanded in the presence of doxycycline and were then split into doxy (+) and

no doxy media (–) at passage 3. E2F3 levels were measured at the end of each passage. After passage 5, half of the “no doxy” MEFs were reversed back into doxycycline containing media (R).

Figure 3-6. E2F3 expression is repressed in *e2f3$^{tre/tre}$;tTS* tissues after removal of doxycycline.

e2f3$^{tre/tre}$;tTS/tTS mice grown in the presence of doxycycline were removed from doxycycline treatment at weaning (three weeks of age). Graphs show Taqman analysis of *e2f3a* (A) and *e2f3b* (B) mRNA expression in selected organs after removal of doxycycline. *e2f3* is efficiently repressed in all tested tissues.

Figure 3-7. Repression of E2F3 slows down cell proliferation

e2f3$^{tre/tre}$;tTS MEFs were cultured with or without doxycycline (doxy removed on passage 3). After passage 5, half of the cells grown without doxy were reversed back to doxy. Repression of *e2f3* slows down cell proliferation, however, proliferation rates go back to normal when *e2f3* expression is restored.

Figure 3-8. *e2f3* repression is not lethal in adult *e2f3$^{tre/tre}$;tTS/tTS* mice.

e2f3$^{tre/tre}$;tTS/tTS mice were kept in the presence of doxycycline or removed from doxycycline at weaning. Graph shows how long different cohorts (each

line is a separate cohort) have been with or without doxycycline. Mice kept off doxycycline are healthy and viable, despite having no E2F3 for weeks.

Figure 3-9. *e2f3* is repressed in *e2f3$^{tre/tre}$;tTS;EμMyc* tumors after removal of doxycycline.

A) Experimental design: *e2f3$^{tre/tre}$;tTS;EμMyc* mice were allowed to develop tumors. Tumors were then collected and transplanted into wild type recipients that are kept on or off doxycycline.

B) Taqman analysis of *e2f3* mRNA expression in three independent *e2f3$^{tre/tre}$;tTS;EμMyc* tumors.

C) Taqman analysis of *e2f3* expression in spleens of two wild type recipient mice one week after they were transplanted with tumor #1 (shown on B). One mouse was kept on doxycycline and the other off doxycycline. The Taqman probes used detect only mRNA from the tumor cells. (∗)= No *e2f3a* was detected in off-doxy mouse.

Figure 3-10. *e2f3* repression does not affect survival of mice transplanted with lymphoma.

A) Wild type recipient mice were transplanted with an *e2f3$^{tre/tre}$;tTS;EμMyc* tumor. Recipient mice were kept on or off doxycycline, as indicated. Their survival after transplant is plotted.

B) Taqman analysis of *e2f3* mRNA levels in tumors from recipient mice kept on or off doxycycline, as indicated. Each pair of bars is a separate tumor (total of 11 tumors). (∗)= no *e2f3a* mRNA detected.

Figure 3-1

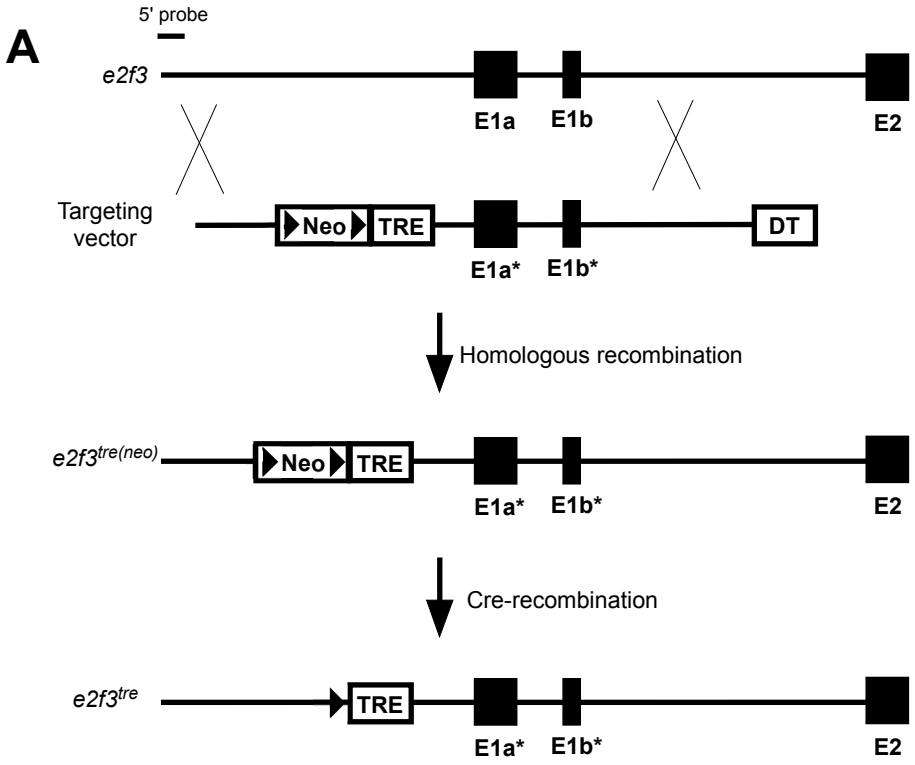
A
5' probe
e2f3
E1a
E1b
E2
Targeting vector
Neo
TRE
DT
E1a*
E1b*
Homologous recombination
e2f3tre(neo)
Neo
TRE
E1a*
E1b*
E2
Cre-recombination
e2f3tre
TRE
E1a*
E1b*
E2

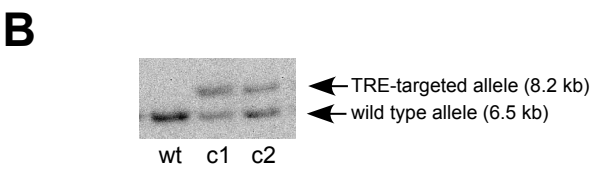
B
TRE-targeted allele (8.2 kb)
wild type allele (6.5 kb)
wt
c1
c2

Figure 3-2

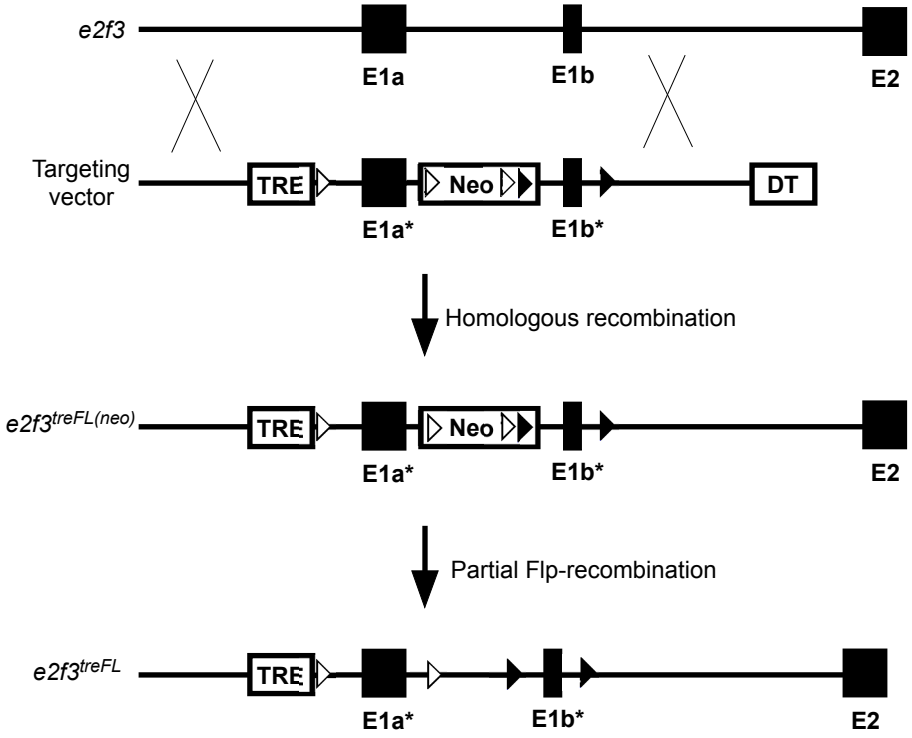
e2f3
E1a
E1b
E2
Targeting vector
TRE
Neo
DT
E1a*
E1b*
Homologous recombination
e2f3treFL(neo)
TRE
Neo
E1a*
E1b*
E2
Partial Flp-recombination
e2f3treFL
TRE
E1a*
E1b*
E2

Figure 3-3

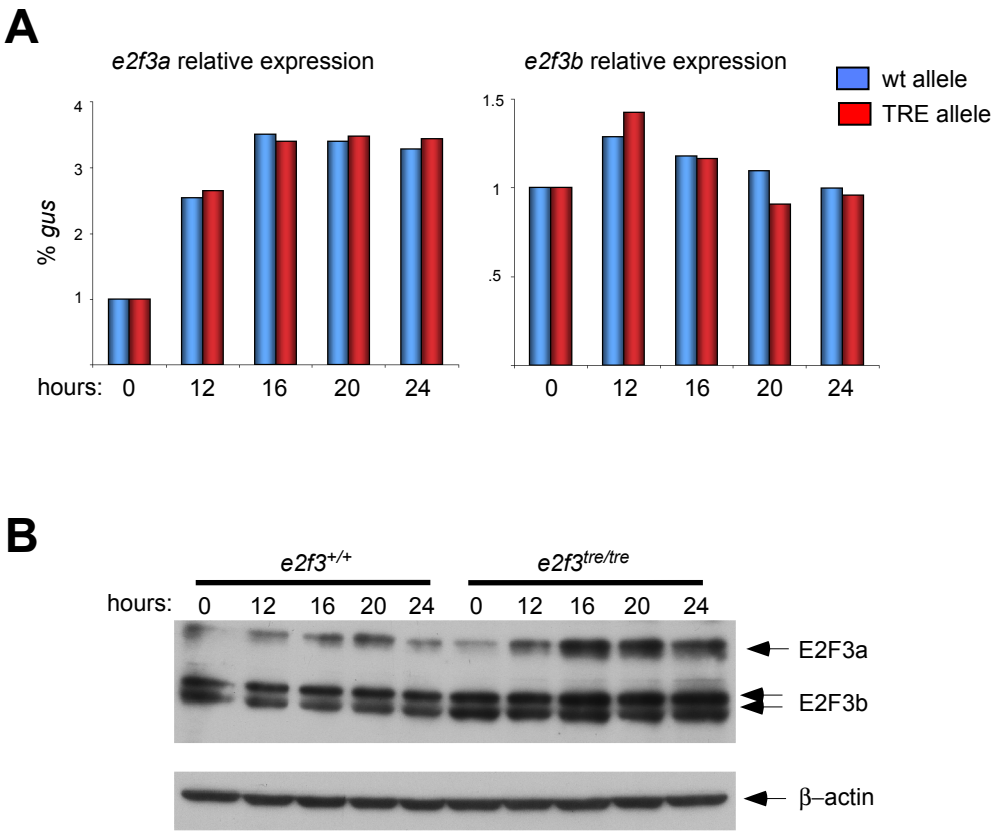
A
e2f3a relative expression
e2f3b relative expression
wt allele
TRE allele
% gus
4
3
2
1
1.5
1
.5
hours: 0 12 16 20 24
0 12 16 20 24
B
e2f3+/+
e2f3tre/tre
hours: 0 12 16 20 24 0 12 16 20 24
E2F3a
E2F3b
β–actin

Figure 3-4.

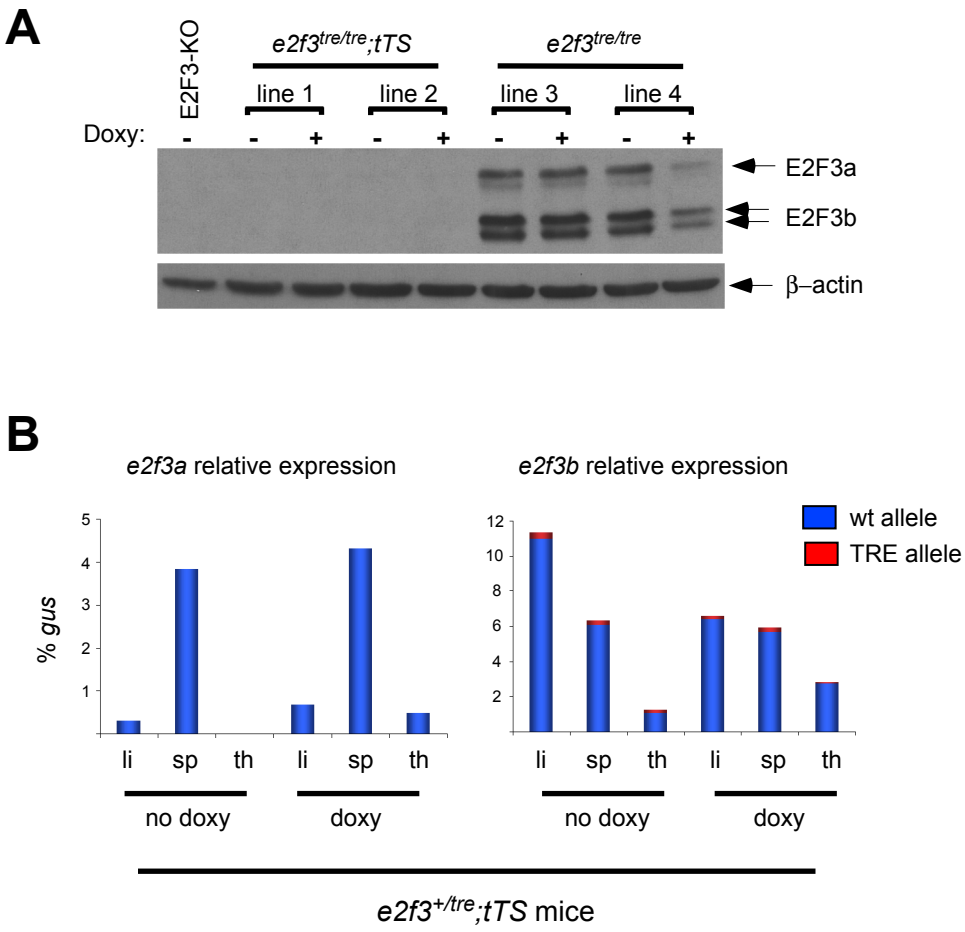
A
E2F3-KO
e2f3tre/tre;tTS
e2f3tre/tre
line 1
line 2
line 3
line 4
Doxy:
- - + - + - + - +
E2F3a
E2F3b
β–actin
B
e2f3a relative expression
e2f3b relative expression
wt allele
TRE allele
% gus
5
4
3
2
1
12
10
8
6
4
2
li sp th li sp th
no doxy
doxy
li sp th li sp th
no doxy
doxy
e2f3+/tre;tTS mice

Figure 3-5.

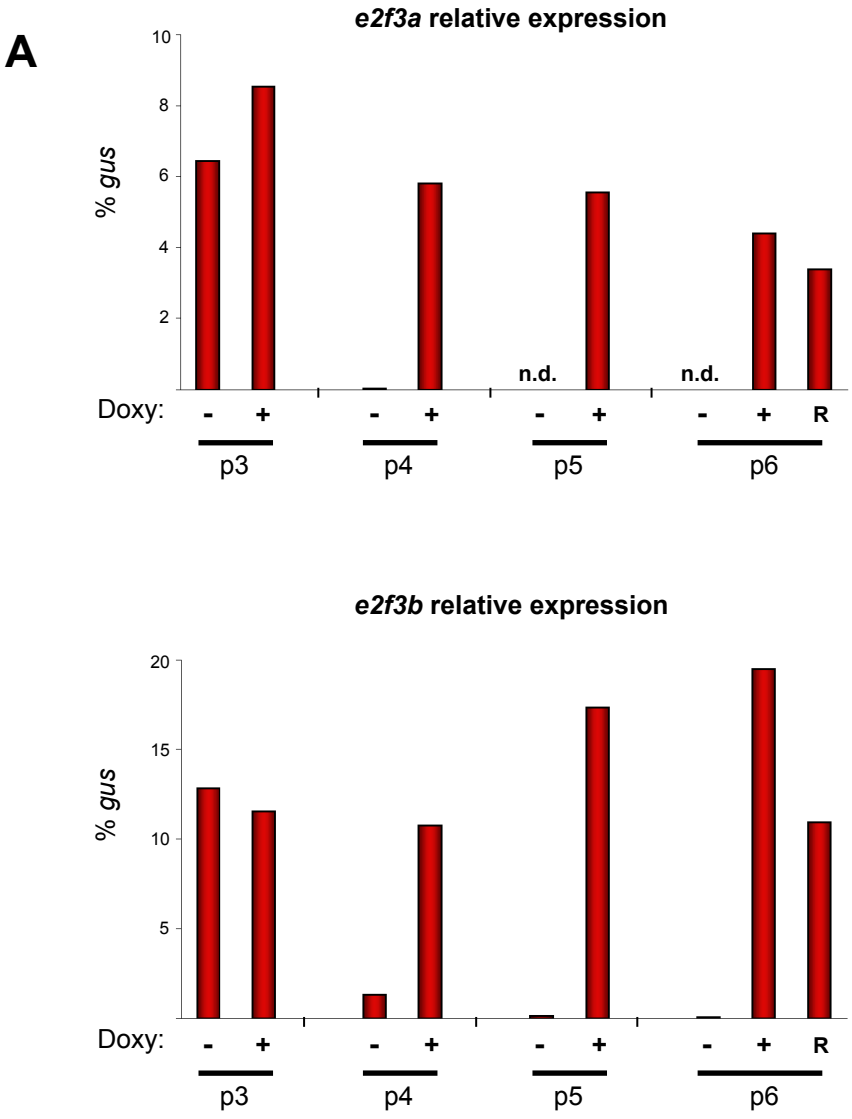
A
e2f3a relative expression
% gus
10
8
6
4
2
n.d.
n.d.
Doxy:
- + - + - + - + R
p3
p4
p5
p6
e2f3b relative expression
% gus
20
15
10
5
Doxy:
- + - + - + - + R
p3
p4
p5
p6

Figure 3-5 (cont).

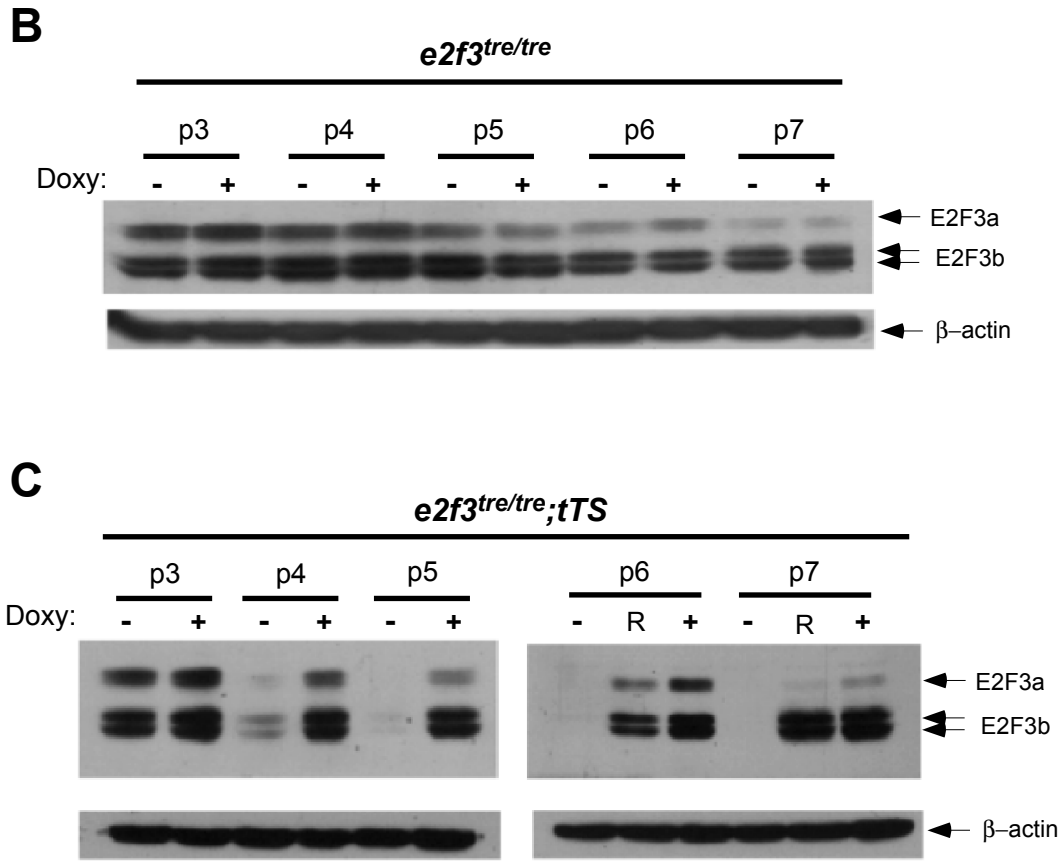

Figure 3-6

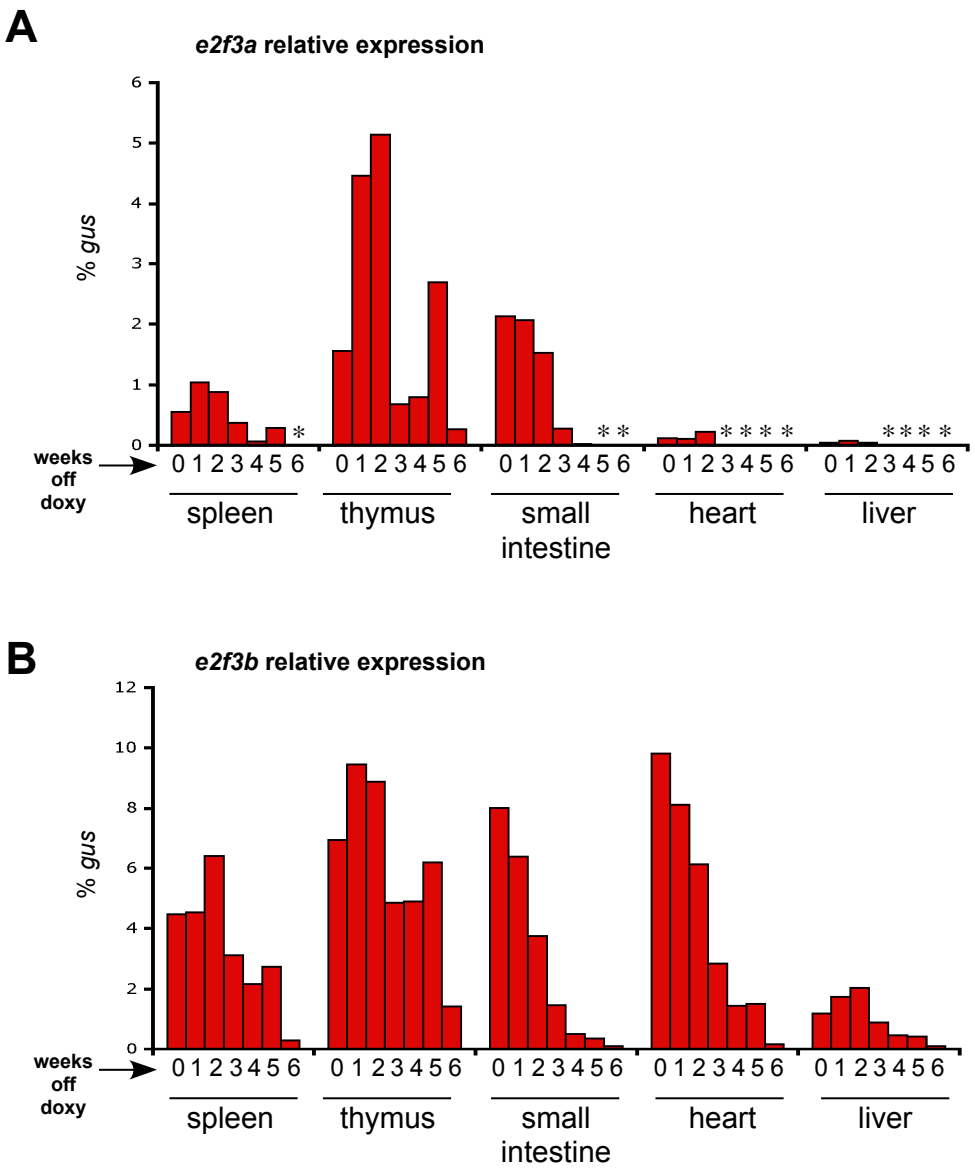
A
e2f3a relative expression
% gus
6
5
4
3
2
1
0
weeks off doxy
0 1 2 3 4 5 6
spleen
thymus
small intestine
heart
liver
B
e2f3b relative expression
% gus
12
10
8
6
4
2
0
weeks off doxy
0 1 2 3 4 5 6
spleen
thymus
small intestine
heart
liver

Figure 3-7.

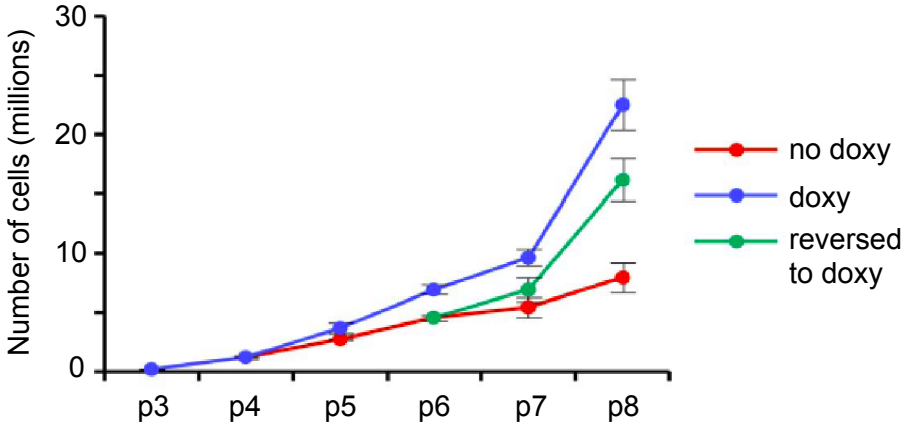
Number of cells (millions)
30
20
10
0
p3
p4
p5
p6
p7
p8
no doxy
doxy
reversed to doxy

Figure 3-8.

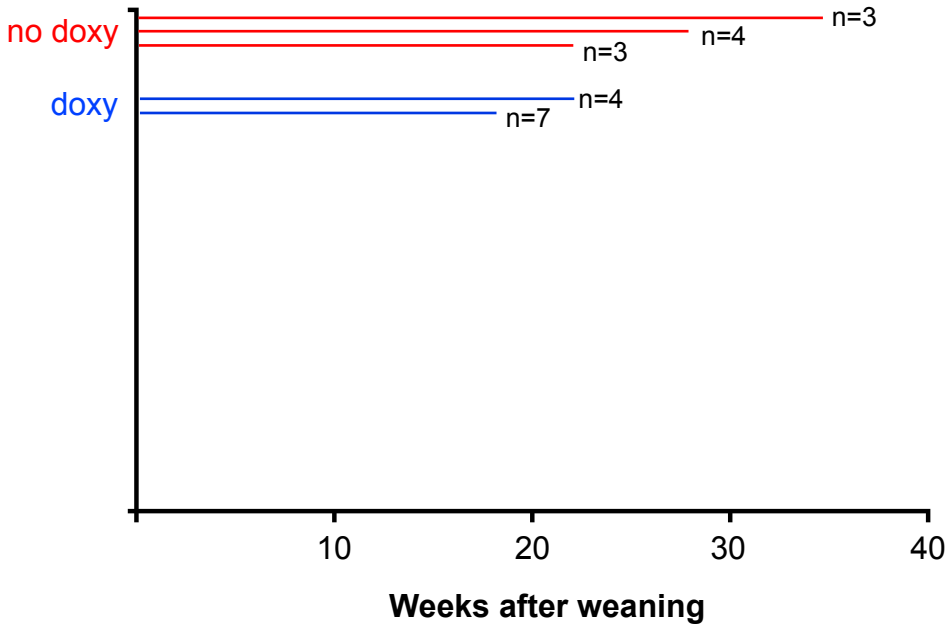

Figure 3-9.

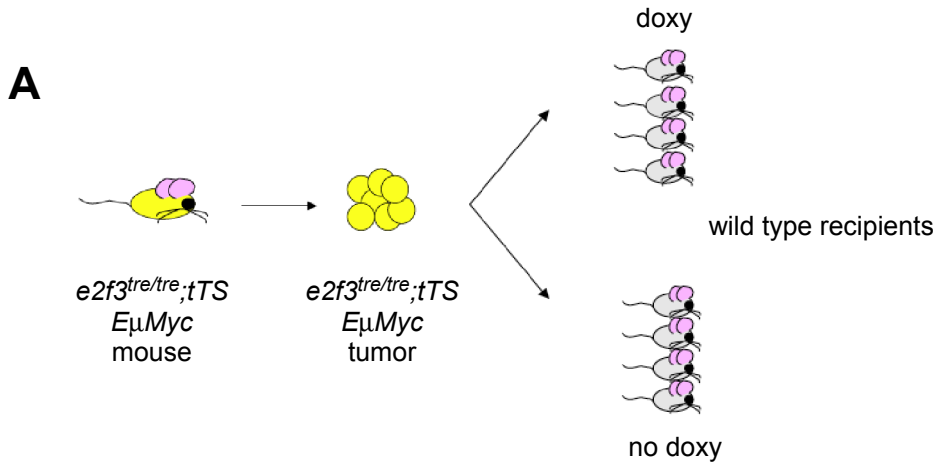
A
doxy
wild type recipients
no doxy
e2f3tre/tre;tTS
EμMyc
mouse
e2f3tre/tre;tTS
EμMyc
tumor

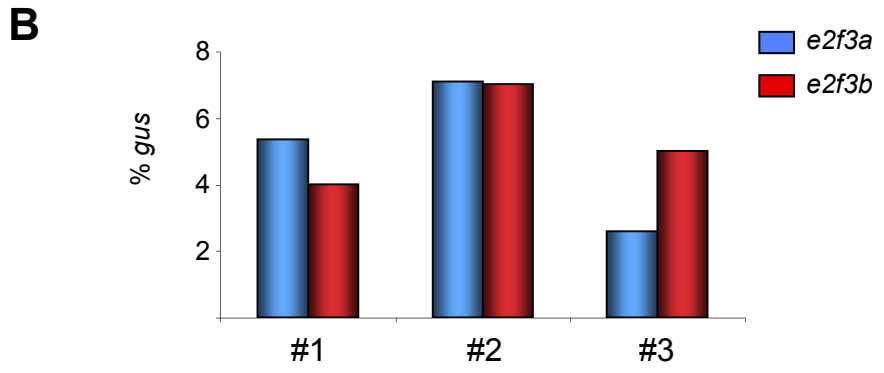
B
e2f3a
e2f3b
% gus
8
6
4
2
#1
#2
#3

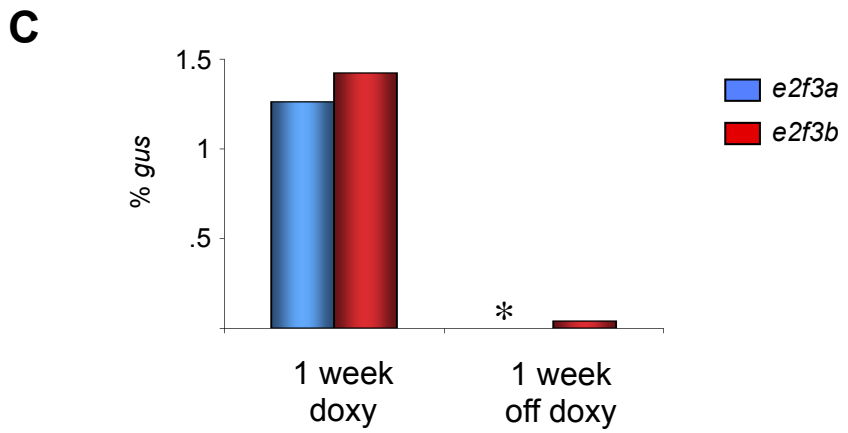
C
e2f3a
e2f3b
% gus
1.5
1
.5
*
1 week
doxy
1 week
off doxy

Figure 3-10.

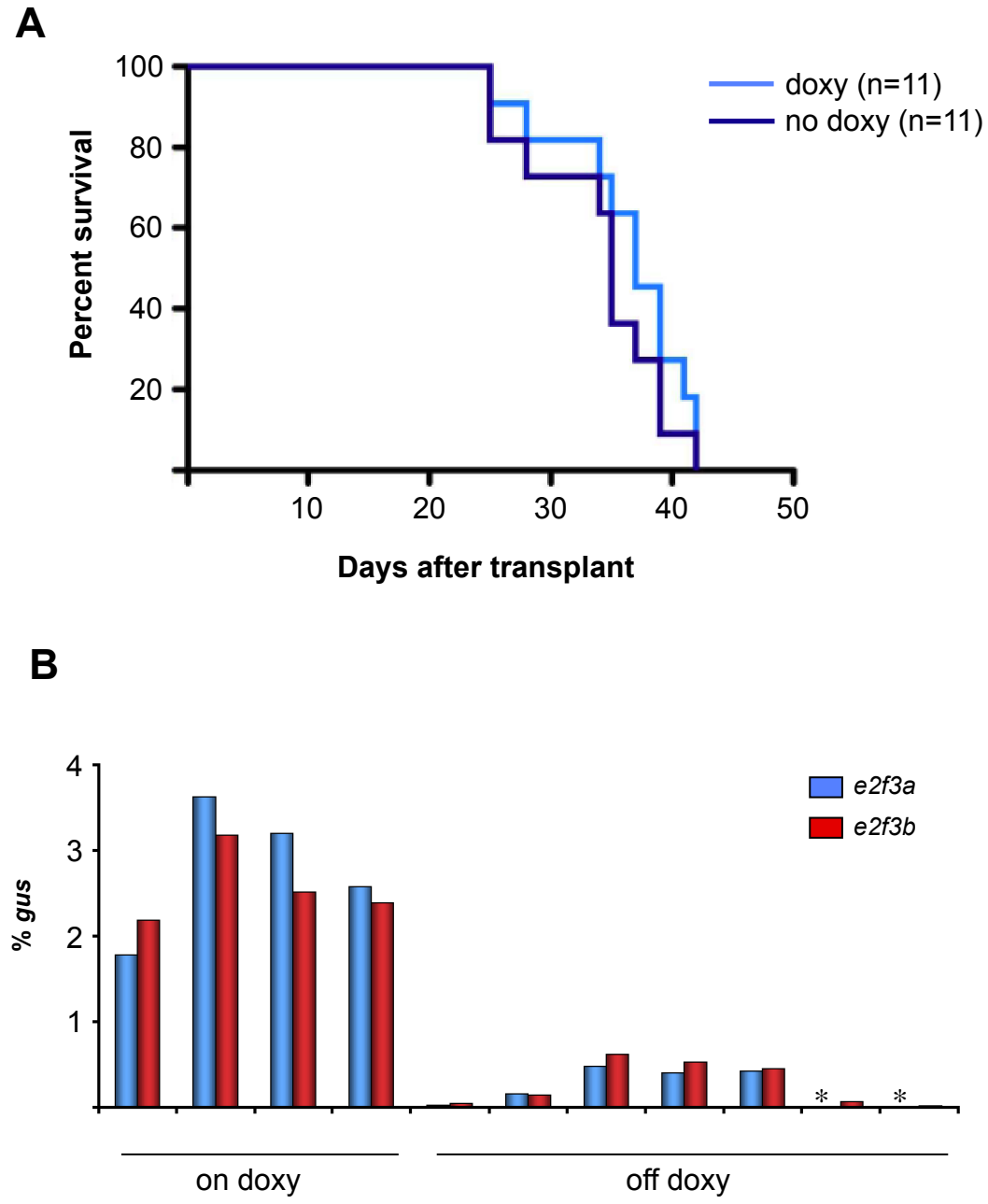
A
100
80
60
40
20
Percent survival
doxy (n=11)
no doxy (n=11)
10
20
30
40
50
Days after transplant
B
4
3
2
1
% gus
e2f3a
e2f3b
*
*
on doxy
off doxy

CHAPTER 4

Discussion and future directions

MdmX inhibition is a viable therapeutic strategy to restore p53 function in tumors.

MdmX is a critical negative regulator of p53 (Mancini et al. 2010; Marine and Jochemsen 2005; Marine et al. 2007; Wade and Wahl 2009) necessary to restrain the lethal consequences of unbridled p53 activity during normal development (Parant et al. 2001; Migliorini et al. 2002; Francoz et al. 2006; Grier et al. 2006; Xiong et al. 2006). However, the embryonic lethality of p53-competent MdmX-null mice has confounded genetic analysis of the role played by MdmX in governing p53 activity in adult tissues. Here, we have used a switchable p53 mouse model, in which endogenous p53 function can be systemically enabled or disabled at will (Christophorou et al. 2005), to establish the consequences of restoring p53 in adult *mdmX*$^{-/-}$ tissues. Our data indicate that p53 is spontaneously active in *mdmX*$^{-/-}$ adult mouse tissues, triggering induction of p53 target genes in all tested organs and widespread apoptosis in radiosensitive tissues. Moreover, sustained systemic p53 function in such *mdmX*$^{-/-}$ mice is ultimately lethal. This unequivocally establishes MdmX, like Mdm2 (Ringshausen et al. 2006), as critically and continuously required to rein in precocious p53 activity in normal adult tissues.

Nonetheless, while both Mdm2 and MdmX serve as constitutive buffers against untoward p53 activity in adult tissues *in vivo*, their roles are quantitatively and qualitatively quite distinct. Both the anti-proliferative gene *cdkn1a* and pro-apoptotic gene *puma* are indiscriminately induced in all *mdm2*$^{-/-}$ tissues following

acute p53 restoration, irrespective of whether the cells within that tissue then undergo apoptosis or viable cell cycle arrest (Ringshausen et al. 2006). By contrast, p53 target gene induction is more selective in tamoxifen-treated *mdmX*$^{-/-}$;*p53*$^{KI/-}$ tissues: *cdkn1a* is still induced in most *mdmX*$^{-/-}$ tissues (with the notable exception of intestinal epithelium) but in the main *puma* is up-regulated only in those *mdmX*$^{-/-}$ tissues that undergo apoptosis. Given the evidence suggesting that *cdkn1a* and *puma* are induced by different threshold levels of p53 activity (Morachis et al. 2010; Vousden and Prives 2009), the most plausible explanation for such differential target gene induction is the markedly lower overall p53 activity elicited by p53 restoration in *mdmX*$^{-/-}$;*p53*$^{KI/-}$ tissues compared with that in their *mdm2*$^{-/-}$ counterparts. Presumably, it is this higher level of p53 activity in *mdm2*-deficient tissues that is responsible for the far more precipitous and deleterious effects of p53 restoration in *mdm2*$^{-/-}$ tissues. Of note, our observations are inconsistent with a simple binary model whereby loss of Mdm2 directs p53 to induce apoptosis while loss of MdmX directs p53 to engage growth arrest (Barboza et al. 2008). For example, both the pro-apoptotic gene *puma* and overt apoptosis are potently induced in classically radiosensitive adult tissues of *p53*$^{KI/-}$;*mdmX*$^{-/-}$ mice after p53 restoration. And conversely, while *puma* is potently induced by p53 restoration even in radio-resistant *mdm2*$^{-/-}$ tissues, no apoptosis occurs even if those tissues are forced to proliferate (Ringshausen et al. 2006). Hence, the proclivity of any adult tissue to undergo p53-induced apoptosis appears to be an intrinsic attribute of that tissue and not the purview of either Mdm2 or MdmX.

Restoration of p53 function has been vigorously pursued as a potential therapeutic approach to treat cancers and, moreover, has recently been shown to be therapeutically beneficial in several preclinical mouse cancer models (Martins et al. 2006; Ventura et al. 2007; Xue et al. 2007). Accordingly, numerous efforts have focused on blocking endogenous inhibitors of p53, in the main Mdm2, as a strategy for re-activating p53 in tumors (Issaeva et al. 2004; Vassilev et al. 2004; Shangary et al. 2008; Sun et al. 2008; Canner et al. 2009; Hedstrom et al. 2009). Unfortunately, efficient inhibition of Mdm2 triggers p53 not only in tumor cells but also in all normal cells, eliciting rapid, irreversible and eventually lethal deterioration of sensitive tissues (Ringshausen et al. 2006). By contrast, our data indicate that transient inhibition of MdmX is a far less intrinsically toxic and hazardous therapeutic strategy for re-activating p53: while transient p53 activity in the absence of MdmX does damage lymphoid organs and bone marrow, it has unexpectedly mild effects on intestinal epithelium, which is arguably the most critical tissue limiting therapeutic toxicity since its failure is rapidly and irreversibly fatal due to fluid loss and bacterial incursion. Presumably as a corollary of this remarkable preservation of intestinal integrity, all other sequelae arising from transient p53 activity in the absence of MdmX are reversible, with all mice recovering and thereafter living long-term. Significantly, absence of MdmX augments the therapeutic impact of restoring p53 function in treating lymphoma. This, together with the muted toxicity of p53 in the absence of MdmX and the complete reversibility of its pathological side effects, support the

notion that MdmX inhibition is a feasible strategy for restoring p53 in select tumors.

Increasing evidence now implicates p53 in the regulation of adult stem cell homeostasis. Most notably, chemical inhibition or genetic ablation of p53 elicits defects in stem cell self-renewal and increased proliferation rates that eventually lead to an expansion of both hematopoietic and neural stem cells (Leonova et al. 2010) (TeKippe et al. 2003; Meletis et al. 2006; Liu et al. 2009). By showing that preternatural p53 activity causes attrition of hematopoietic stem cells, our data now add to the emerging view that the converse is also true (Abbas et al. 2010; Liu et al. 2009). However, in keeping with the very different toxicities associated with p53 activity in the absence of MdmX versus Mdm2, the severity and rapidity of stem cell attrition was very different in each case. Even fleeting p53 restoration in *mdm2*-deficient mice rapidly and irreversibly wiped out HSCs, together with any capacity of the bone marrow to regenerate when p53 function was subsequently de-activated. By contrast, absence of MdmX provoked a much milder and protracted erosion of HSCs that allowed for complete bone marrow regeneration and recovery of animals even after extended periods of p53 restoration. This difference has important practical implications. Although our data indicate a previously unappreciated role for both Mdm2 and MdmX in buffering p53 activity in adult hematopoietic stem cells, they also indicate that aggressive pharmacological inhibition of Mdm2 rapidly and irreversibly depletes stem cell pools whereas efficient MdmX inhibition does not. This might also be true for stem cells of other tissues as suggested by our observation that intestinal

epithelia were relatively unaffected by p53 restoration in the absence of MdmX compared to restoration in the absence of Mdm2, indicating that intestinal stem cells continue to regenerate and maintain epithelial integrity in *mdmX*$^{-/-}$ mice after p53 restoration, but not in their *mdm2*$^{-/-}$ counterparts.

Ultimately, however, the capacity of p53 restoration therapy to prolong overall survival is limited by the emergence of resistant clones in tumors that are deficient either in p53 itself or in the upstream signals that engage p53, most notably p19^{ARF} (Junttila et al. 2010; Martins et al. 2006). Moreover, our data show that such resistant secondary tumors do indeed arise following p53 restoration in MdmX-deficient mice. Given that such p53 pathway-defective cells presumably pre-exist in the *EμMyc* tumors prior to the initial p53 restoration and it is to these exapted clones that the mice eventually succumb, how might inactivation of MdmX enhance the therapeutic potential of p53 restoration? One possibility is suggested by our immunoblot analysis, which indicates that a low-level of p53 remains in the resistant tumors. Since deletion of the *p53* gene is the mechanism of secondary resistance to tamoxifen in such recurring tumors, such low-level p53 presumably indicates the persistence of a minor remnant population of p53-positive cells. Of note, the residual level of p53 in recurring MdmX-deficient tumors is lower than that in their MdmX-competent counterparts, likely indicating that fewer p53-competent tumor cells survive the initial p53 restoration. A better initial “kill” of tumor cells in the absence of MdmX would be consistent with the extended survival of the tamoxifen-treated *mdmX*-deficient mice. It has also recently emerged that tumors can evade p53-mediated tumor suppression by

failing to breach the signaling threshold required to trigger the p53 pathway (Junttila et al. 2010; Sarkisian et al. 2007; Murphy et al. 2008). In such cases, inhibiting MdmX has the potential to lower the p53-activating threshold, so engaging the p53 pathway in a tumor-selective manner. The recent identification of the first small-molecule inhibitor of MdmX (Reed et al. 2010) may therefore be an important step forward in the genesis of novel therapies that are truly tumor-specific.

***e2f3$^{tre/tre}$;tTS* mice validate tet-repressor system as a novel switchable mouse model.**

E2F3 has a well-established role as a driver of cellular proliferation and is essential for embryonic development. Furthermore, it is an important component of tumor suppressor pathways such as the Rb and p19^{ARF}/p53 pathways (Aslanian et al. 2004). In fact, E2F3 has been reported to be overexpressed in many types of cancer (Ziebold et al. 2003; Feber et al. 2004; Foster et al. 2004; Grasemann et al. 2005). However, traditional knockout genetic strategies preclude the study of E2F3 biology in adult tissues and tumors because of embryonic lethality of E2F3-null mice. Although our lab has successfully used estrogen moieties to achieve regulation of genes in adult tissues (Christophorou et al. 2005), this strategy cannot be applied to E2F3 because estrogen receptor inducers are abortive. To solve these problems, we developed and implemented a new genetic strategy, dubbed “tet-repressor targeting”, that allows control of endogenous genes in adult tissues and tumors via a tetracycline sensitive trans-

repressor. It consists of the insertion of a 300 base pair DNA fragment (commonly known as TRE) into an endogenous gene, which serves as a binding site for a dominant tetracycline-sensitive transcription repressor, called tTS (tetracycline trans-silencer), which functions as a molecular switch. In the presence of doxycycline (or other tetracycline antibiotics) tTS is inactive. In the absence of doxycycline tTS becomes active, binds the TRE and represses expression of the targeted gene.

We have applied this new technology to the *e2f3* gene and have generated *e2f3*$^{tre/tre}$*;tTS* mice. Indeed, *e2f3* was efficiently repressed by tTS in the absence of doxycycline both in *e2f3*$^{tre/tre}$*;tTS* MEFs *in vitro* and in *e2f3*$^{tre/tre}$*;tTS* adult mice *in vivo,* allowing us for the first time to systemically eliminate expression of a gene in adult mice. We show that *e2f3*$^{tre/tre}$*;tTS* adult mice are healthy and viable long after E2F3 has been completely repressed, which is the first reported example of a gene that is required for embryogenesis, but is dispensable for adult life. Beyond the gained insights on E2F3 function in adult tissues, however, validation of tet-repressor targeting represents a significant advancement over traditional mouse genetics. Because this technology can be applied to any gene, tet-repressor targeting has enormous potential for the study of gene function in adult tissues and tumors. In fact, we have already applied this technology to the *c-Myc* and *p73* genes. Studies on those mice will further validate tet-repressor targeting as a new tool for gene manipulation in adult tissues and tumors.

Optimization of *e2f3* repression by tTS *in vivo* has proven to be challenging. Although repression eventually takes place, it does so few weeks after doxycycline removal: the timing of the repression is therefore less than ideal. That being said, we think the slow kinetics of repression are not an intrinsic property of tTS, but rather a consequence of slow clearance of doxycycline from the body. Indeed, *e2f3* was quickly repressed in *e2f3*$^{tre/tre}$*;tTS;Eμ-Myc* tumors after only one week following transplantation into doxycycline-free recipient mice, strongly suggesting that repression can happen quickly if only doxycycline could be cleared quickly as well. Nonetheless, we are currently pursuing two additional avenues for optimization of tet-repressor targeting. First, we have now grown *e2f3*$^{tre/tre}$*;tTS/tTS* mice in the presence of tetracycline (100μg/ml, in drinking water) instead of doxycycline. Tetracycline has a shorter half-life than doxycycline (6-8 hours versus 18-22 hours, respectively) and is therefore predicted to be cleared faster from the body. We expect *e2f3* to be repressed much faster in these mice after removal of tetracycline. Second, we are developing a reverse tTS repressor (rtTS). The goal is to fuse the tet-sensitive domain of rtTA with the trans-silencing domain of tTS. The resulting rtTS repressor would now be inactive in the absence of doxycycline (like rtTA) and repress targeted genes when doxycycline is provided. rtTS would eliminate the need to wait for doxycycline to clear in order for the repression to take place. Administration of doxycycline would now switch to the repressive state, which we predict would happen much faster (hours instead of weeks, similar to rtTA). Construction of the rtTS repressor is arguably the single most important

improvement we can make in order to promote widespread use of this technology.

Interestingly, despite the critical requirement of E2F3 for completion of embryogenesis, repression of E2F3 in adult mice had no impact on viability. Similarly, E2F3 repression did not affect tumor progression in a transplant mouse model of lymphoma. In both cases, either E2F3 no longer provides an essential function, or E2F3 loss can be compensated by the other activating E2F transcription factors, E2F1 and E2F2. To address these questions, we have now crossed *e2f3$^{tre/tre}$;tTS* mice with E2F1 and E2F2 null mice to generate *e2f1$^{-/-}$;e2f2$^{-/-}$;e2f3$^{tre/tre}$;tTS* mice. We have also crossed these mice with *EμMyc* mice to generate *e2f1$^{-/-}$;e2f2$^{-/-}$;e2f3$^{tre/tre}$;tTS;EμMyc* mice. These mice will allow us to answer not only whether E2F1 and E2F2 were compensating for E2F3 repression, but they would also allow us to answer the more profound question of whether global activating-E2F function is required for adult viability and for tumor maintenance and progression. Indeed, recent studies have demonstrated that activating E2F proteins are more redundant than previously thought (Tsai et al. 2008). Accordingly, the case could be made that repressing E2F3 in *e2f1$^{-/-}$;e2f2$^{-/-}$;e2f3$^{tre/tre}$;tTS* mice is a valid model for repressing global activating-E2F function. We can now assess whether systemic loss of activating-E2F function is tolerated or lethal in adult mice. More importantly, repression of E2F3 in *e2f1$^{-/-}$;e2f2$^{-/-}$;e2f3$^{tre/tre}$;tTS;EμMyc* tumors will allow us to assess whether inhibition of global activatin-E2F function has any effect in these tumors and whether this confers

any therapeutic benefit. Only tet-repressor targeting technology makes it possible to address these questions in adult mice.

CHAPTER 5:

Materials and Methods

Construction of *e2f3^{tre}* and *e2f3^{treFL}* targeting vectors.

To contruct the *e2f3^{tre}* targeting vector, a genomic DNA fragment that contained the *e2f3* promoter, exons 1a and 1b, as well as intronic sequences was subcloned into pBlueScript. The TRE fragment and a floxed Neo cassette (for selection) were introduced into a KpnI site just upstream of the E2F3a promoter. Silent mutations were introduced in both exon 1a and 1b, to distinguish mRNA derived from the targeted allele from mRNA derived from the wild type allele. A diphtheria toxin gene was also inserted for negative selection. A map of the *e2f3^{tre}* targeting vector is shown on Figure 3-1. The same *e2f3* genomic DNA was used to construct the *e2f3^{treFL}* targeting vector. The TRE sequence was inserted in the same KpnI site, but a flrted Neo cassette was placed further downstream instead. Additional *loxP* and *FRT* sites were inserted, as needed. The same silent mutations were introduced and the same diphtheria toxin gene was used. A map of the *e2f3^{treFL}* targeting vector is shown on Figure 3-2.

Generation of *e2f3^{tre}* and *e2f3^{treFL}* mice.

e2f3^{tre} and *e2f3^{treFL}* targeting vectors were linearized and electroporated into 129/1 embryonic stem (ES) cells. G148 resistant clones were screened by PCR and by Southern blot for correct homologous recombination. Positive clones were expanded and validated by Southern blot using both 5' and 3' external probes. To generate *e2f3^{tre}* mice, a positive *e2f3^{tre}* ES cell clone was transiently transfected with a vector that expressed *Cre* recombinase, in order to excise the Neo cassette. A clone that excised the Neo cassette was then introduced into

C57BL/6 derived blastocysts to generate chimeric mice. To generate *e2f3*^{treFL} mice, a positive *e2f3*^{treFL} ES cell clone was transiently transfected with a vector that expressed low levels of *Flp* recombinase, in order to excise the Neo cassette. A clone that excised the Neo cassette, but not exon 1a (partial recombination) was identified by PCR and was introduced into C57BL/6 derived blastocysts to generate chimeric mice. *e2f3*^{tre} and *e2f3*^{treFL} chimeric mice were back-crossed to C57BL/6 mice and germline transmission was confirmed by PCR.

Cell culture.

Mouse embryonic fibroblasts (MEFs) were isolated on embryonic day 13.5 and cultured in Dulbecco's modified Eagle medium (Invitrogen) supplemented with 10% fetal bovine serum (Invitrogen) and 1% penicillin /G-streptomycin sulfate (Invitrogen). To restore p53 *in vitro* in *p53*$^{KI/-}$ MEFs, cells were exposed to 100 nM 4-hydroxytamoxifen (Sigma, H7904). Nutlin-3a was purchased from Cayman Chemical Company (Cat. No. 18585). When indicated, *e2f3*^{tre} MEFs were exposed to 2 μg/ml doxycycline (Sigma D9891).

Lymphoma cell cultures were established and maintained as described (Martins et al. 2006).

Genetically engineered mice.

p53ER^{TAM}*KI (p53*$^{KI/KI}$*)* mice (Christophorou et al. 2005) were crossed with *p53*$^{-/-}$ (Jacks et al. 1994), *mdmX*$^{-/-}$ (Parant et al. 2001), *mdm2*$^{-/-}$ (Montes de Oca

Luna et al. 1995), and *Eμ-myc* mice (Adams et al. 1985) to generate the appropriate genotypes. *e2f3*^{tre} mice were crossed to *β-actin-tTS* (unpublished) and *Eμ-myc* mice to generate the appropriate genotypes. All animals were kept under SPF conditions and all experimental procedures adhered to approved UCSF IACUC protocols.

***In vivo* studies with mice.**

To restore p53 in *p53*^{KI} mice, mice were injected intraperitoneally with 100 μl of 10 mg/ml tamoxifen (Sigma, T5648) in peanut oil, at the indicated frequencies. Where appropriate, mice were injected with a single bolus of 100 μl of 10 mg/ml BrdU (Sigma, B5002) 2 hours prior to sacrifice. When appropriate, *e2f3*^{tre} mice were administered doxycycline (Sigma D9891) in their drinking water (at the indicated concentrations). To allow for *e2f3* repression mice were removed from doxycycline regimen and put on regular water.

For tumor studies, wild type mice were given 4 Gy irradiation 4 hours prior to tail-vein transplantation of lymphomas using a Mark 1-68 ^{137}Cesium source (1.972 Gy/min). Lymphoma cells were thawed immediately before use, washed, counted and injected intravenously (10^6 cells/mouse in 100 μl of PBS) into irradiated mice. Statistical analysis of survival was performed with the Kaplan-Meier log-rank test.

Taqman Analysis

Total RNA was isolated with Trizol™ (Invitrogen, cat no. 15596026) and DNase treated (Invitrogen, cat no. 18065-015) prior to reverse transcription (iScript, Bio-Rad, cat no. 170-8891). Taqman analysis was performed as previously described (Christophorou et al. 2005). All data were normalized to *gus* expression.

Immunoblotting

Proteins were extracted from organs and cells using standard RIPA buffer. Protein lysates (50-100 μg) were fractionated on SDS polyacrylamide gels and blotted on to PVDF membranes (Immobilon-P, Millipore, IPVH00010). The antibodies used were anti-ER (Santa Cruz, sc-542), anti p21 (BD Pharmingen, cat no. 556431), anti-$p19^{ARF}$ (Novus, clone C3), anti-E2F3 (from J. Lees lab, non commercially available) and anti-β-actin (AC-15, Sigma).

Immunohistochemistry

All collected organs were fixed overnight, washed, processed and embedded in paraffin. BrdU staining and TUNEL were performed using kits (ROCHE, ref 11299964001 and Millipore, cat no. S1760, respectively), following the manufacturer's instructions. Anti-Ki-67 antibody was from NeoMarkers (SP6).

Flow cytometry

Leg, hip and arm bones from individual mice were pooled and crushed to harvest bone marrow (BM) cells. Following lysis of erythrocytes with ACK, BM cells were separated from bone residue and dead cells by FICOL gradient centrifugation. BM cells were then re-suspended in Hank's buffered saline (HBSS) containing 2% heat-inactivated FBS (Hyclone) and total viable cells numbers quantitated using a VI-CELL XR (Beckman-Coulter) imaging hemacytometer. For HSC analysis, 10 x 10^6 BM cells were incubated with rat un-conjugated lineage antibodies (CD3, CD4, CD5, CD8, B220, Ter119, Mac1, Gr1), stained with PE-Cy5 conjugated goat anti-rat IgG (Caltag) and blocked with rat IgG (Sigma). Cells were then stained with Sca1-PB, CD150-PE and CD48-APC (Biolegend). For mature analysis 1 x10^6 cells were stained for B-Cells (B220-APC, CD19-PE (ebioscience) and myeloid cells (Mac1-PE-Cy7, Gr1-PB (ebioscience)). After staining, cells were re-suspended in HBSS + 2% FBS and 1 μg/ml propidium iodide for dead cell exclusion and analyzed on an LSRII (Becton Dickenson).

Southern Blot Analysis

For Southern analysis, 10 μg of genomic DNA per sample was digested with the appropriate restriction enzyme, fractionated in a 0.7% agarose gel, transferred to a nylon membrane and hybridized with ^{32}[P] labeled probe (Rediprime II RPN 1633, Amersham). The p53 probe was generated by PCR with the following primers: 5'-ggtaccttatgagccacccgagg (forward) and 5'-cgaacctcaaagctgtcccgtcc

(reverse). The E2F3 probe was generated by PCR with the following primers: 5’-atcctgcagctgatcaatgagcaggctgggg (forward) and 5’-atcctgcagacttgttgccaagagc tacacc (reverse).

Statistics

Unpaired *t* test and Kaplan-Meier log-rank test were used to assess statistical difference. Two-tailed p values of <0.05 were considered significant.

REFERENCES

Abbas, H.A., Maccio, D.R., Coskun, S., Jackson, J.G., Hazen, A.L., Sills, T.M., You, M.J., Hirschi, K.K., and Lozano, G. 2010. Mdm2 is required for survival of hematopoietic stem cells/progenitors via dampening of ROS-induced p53 activity. *Cell Stem Cell* **7**(5): 606-617.

Adams, J.M., Harris, A.W., Pinkert, C.A., Corcoran, L.M., Alexander, W.S., Cory, S., Palmiter, R.D., and Brinster, R.L. 1985. The c-myc oncogene driven by immunoglobulin enhancers induces lymphoid malignancy in transgenic mice. *Nature* **318**(6046): 533-538.

Adams, M.R., Sears, R., Nuckolls, F., Leone, G., and Nevins, J.R. 2000. Complex transcriptional regulatory mechanisms control expression of the E2F3 locus. *Mol Cell Biol* **20**(10): 3633-3639.

Aslanian, A., Iaquinta, P.J., Verona, R., and Lees, J.A. 2004. Repression of the Arf tumor suppressor by E2F3 is required for normal cell cycle kinetics. *Genes Dev* **18**(12): 1413-1422.

Barboza, J.A., Iwakuma, T., Terzian, T., El-Naggar, A.K., and Lozano, G. 2008. Mdm2 and Mdm4 loss regulates distinct p53 activities. *Mol Cancer Res* **6**(6): 947-954.

Boesten, L.S., Zadelaar, S.M., De Clercq, S., Francoz, S., van Nieuwkoop, A., Biessen, E.A., Hofmann, F., Feil, S., Feil, R., Jochemsen, A.G. et al. 2006. Mdm2, but not Mdm4, protects terminally differentiated smooth muscle cells from p53-mediated caspase-3-independent cell death. *Cell Death Differ*.

Bracken, A.P., Ciro, M., Cocito, A., and Helin, K. 2004. E2F target genes: unraveling the biology. *Trends Biochem Sci* **29**(8): 409-417.

Canner, J.A., Sobo, M., Ball, S., Hutzen, B., DeAngelis, S., Willis, W., Studebaker, A.W., Ding, K., Wang, S., Yang, D. et al. 2009. MI-63: a novel small-molecule inhibitor targets MDM2 and induces apoptosis in embryonal and alveolar rhabdomyosarcoma cells with wild-type p53. *Br J Cancer* **101**(5): 774-781.

Chen, H.Z., Tsai, S.Y., and Leone, G. 2009. Emerging roles of E2Fs in cancer: an exit from cell cycle control. *Nat Rev Cancer* **9**(11): 785-797.

Chong, J.L., Tsai, S.Y., Sharma, N., Opavsky, R., Price, R., Wu, L., Fernandez, S.A., and Leone, G. 2009. E2f3a and E2f3b contribute to the control of cell proliferation and mouse development. *Mol Cell Biol* **29**(2): 414-424.

Christophorou, M.A., Martin-Zanca, D., Soucek, L., Lawlor, E.R., Brown-Swigart, L., Verschuren, E.W., and Evan, G.I. 2005. Temporal dissection of p53 function in vitro and in vivo. *Nat Genet* **37**(7): 718-726.

Cloud, J.E., Rogers, C., Reza, T.L., Ziebold, U., Stone, J.R., Picard, M.H., Caron, A.M., Bronson, R.T., and Lees, J.A. 2002. Mutant mouse models reveal the relative roles of E2F1 and E2F3 in vivo. *Mol Cell Biol* **22**(8): 2663-2672.

Danielian, P.S., Friesenhahn, L.B., Faust, A.M., West, J.C., Caron, A.M., Bronson, R.T., and Lees, J.A. 2008. E2f3a and E2f3b make overlapping but different contributions to total E2f3 activity. *Oncogene* **27**(51): 6561-6570.

Danovi, D., Meulmeester, E., Pasini, D., Migliorini, D., Capra, M., Frenk, R., de Graaf, P., Francoz, S., Gasparini, P., Gobbi, A. et al. 2004. Amplification of Mdmx (or Mdm4) directly contributes to tumor formation by inhibiting p53 tumor suppressor activity. *Mol Cell Biol* **24**(13): 5835-5843.

DeGregori, J. 2002. The genetics of the E2F family of transcription factors: shared functions and unique roles. *Biochim Biophys Acta* **1602**(2): 131-150.

Feber, A., Clark, J., Goodwin, G., Dodson, A.R., Smith, P.H., Fletcher, A., Edwards, S., Flohr, P., Falconer, A., Roe, T. et al. 2004. Amplification and overexpression of E2F3 in human bladder cancer. *Oncogene* **23**(8): 1627-1630.

Foster, C.S., Falconer, A., Dodson, A.R., Norman, A.R., Dennis, N., Fletcher, A., Southgate, C., Dowe, A., Dearnaley, D., Jhavar, S. et al. 2004. Transcription factor E2F3 overexpressed in prostate cancer independently predicts clinical outcome. *Oncogene* **23**(35): 5871-5879.

Francoz, S., Froment, P., Bogaerts, S., De Clercq, S., Maetens, M., Doumont, G., Bellefroid, E., and Marine, J.C. 2006. Mdm4 and Mdm2 cooperate to inhibit p53 activity in proliferating and quiescent cells in vivo. *Proc Natl Acad Sci U S A* **103**(9): 3232-3237.

Freundlieb, S., Schirra-Muller, C., and Bujard, H. 1999. A tetracycline controlled activation/repression system with increased potential for gene transfer into mammalian cells. *J Gene Med* **1**(1): 4-12.

Gossen, M. and Bujard, H. 2002. Studying gene function in eukaryotes by conditional gene inactivation. *Annu Rev Genet* **36**: 153-173.

Grasemann, C., Gratias, S., Stephan, H., Schuler, A., Schramm, A., Klein-Hitpass, L., Rieder, H., Schneider, S., Kappes, F., Eggert, A. et al. 2005. Gains and overexpression identify DEK and E2F3 as targets of chromosome 6p gains in retinoblastoma. *Oncogene* **24**(42): 6441-6449.

Grier, J.D., Xiong, S., Elizondo-Fraire, A.C., Parant, J.M., and Lozano, G. 2006. Tissue-Specific Differences of p53 Inhibition by Mdm2 and Mdm4. *Mol Cell Biol* **26**(1): 192-198.

Gu, J., Kawai, H., Nie, L., Kitao, H., Wiederschain, D., Jochemsen, A.G., Parant, J., Lozano, G., and Yuan, Z.M. 2002. Mutual dependence of MDM2 and MDMX in their functional inactivation of p53. *J Biol Chem* **277**(22): 19251-19254.

Hanahan, D. and Weinberg, R.A. 2000. The hallmarks of cancer. *Cell* **100**(1): 57-70.

Hedstrom, E., Issaeva, N., Enge, M., and Selivanova, G. 2009. Tumor-specific induction of apoptosis by a p53-reactivating compound. *Exp Cell Res* **315**(3): 451-461.

Humbert, P.O., Verona, R., Trimarchi, J.M., Rogers, C., Dandapani, S., and Lees, J.A. 2000. E2f3 is critical for normal cellular proliferation. *Genes Dev* **14**(6): 690-703.

Issaeva, N., Bozko, P., Enge, M., Protopopova, M., Verhoef, L.G., Masucci, M., Pramanik, A., and Selivanova, G. 2004. Small molecule RITA binds to p53, blocks p53-HDM-2 interaction and activates p53 function in tumors. *Nat Med* **10**(12): 1321-1328.

Jacks, T., Remington, L., Williams, B.O., Schmitt, E.M., Halachmi, S., Bronson, R.T., and Weinberg, R.A. 1994. Tumor spectrum analysis in p53-mutant mice. *Curr Biol* **4**(1): 1-7.

Jackson, M.W., Lindstrom, M.S., and Berberich, S.J. 2001. MdmX binding to ARF affects Mdm2 protein stability and p53 transactivation. *J Biol Chem* **276**(27): 25336-25341.

Junttila, M.R., Karnezis, A.N., Garcia, D., Madriles, F., Kortlever, R.M., Rostker, F., Brown Swigart, L., Pham, D.M., Seo, Y., Evan, G.I., Martins C.P. 2010 Selective activation of p53-mediated tumour suppression in high-grade tumours. *Nature* **468**(7323): 567-571.

Kiel, M.J., Yilmaz, O.H., Iwashita, T., Terhorst, C., and Morrison, S.J. 2005. SLAM family receptors distinguish hematopoietic stem and progenitor cells and reveal endothelial niches for stem cells. *Cell* **121**(7): 1109-1121.

King, J.C., Moskowitz, I.P., Burgon, P.G., Ahmad, F., Stone, J.R., Seidman, J.G., and Lees, J.A. 2008. E2F3 plays an essential role in cardiac development and function. *Cell Cycle* **7**(23): 3775-3780.

Kruse, J.P. and Gu, W. 2009. Modes of p53 regulation. *Cell* **137**(4): 609-622.

Lamartina, S., Silvi, L., Roscilli, G., Casimiro, D., Simon, A.J., Davies, M.E., Shiver, J.W., Rinaudo, C.D., Zampaglione, I., Fattori, E. et al. 2003. Construction of an rtTA2(s)-m2/tts(kid)-based transcription regulatory switch that displays no basal activity, good inducibility, and high responsiveness to doxycycline in mice and non-human primates. *Mol Ther* **7**(2): 271-280.

Laurie, N.A., Donovan, S.L., Shih, C.S., Zhang, J., Mills, N., Fuller, C., Teunisse, A., Lam, S., Ramos, Y., Mohan, A. et al. 2006. Inactivation of the p53 pathway in retinoblastoma. *Nature* **444**(7115): 61-66.

Leone, G., Nuckolls, F., Ishida, S., Adams, M., Sears, R., Jakoi, L., Miron, A., and Nevins, J.R. 2000. Identification of a novel E2F3 product suggests a mechanism for determining specificity of repression by Rb proteins. *Mol Cell Biol* **20**(10): 3626-3632.

Leonova, K.I., Shneyder, J., Antoch, M.P., Toshkov, I.A., Novototskaya, L.R., Komarov, P.G., Komarova, E.A., and Gudkov, A.V. 2010. A small molecule inhibitor of p53 stimulates amplification of hematopoietic stem cells but does not promote tumor development in mice. *Cell Cycle* **9**(7).

Linke, K., Mace, P.D., Smith, C.A., Vaux, D.L., Silke, J., and Day, C.L. 2008. Structure of the MDM2/MDMX RING domain heterodimer reveals dimerization is required for their ubiquitylation in trans. *Cell Death Differ* **15**(5): 841-848.

Liu, Y., Elf, S.E., Miyata, Y., Sashida, G., Liu, Y., Huang, G., Di Giandomenico, S., Lee, J.M., Deblasio, A., Menendez, S. et al. 2009. p53 regulates hematopoietic stem cell quiescence. *Cell Stem Cell* **4**(1): 37-48.

Maetens, M., Doumont, G., Clercq, S.D., Francoz, S., Froment, P., Bellefroid, E., Klingmuller, U., Lozano, G., and Marine, J.C. 2007. Distinct roles of Mdm2 and Mdm4 in red cell production. *Blood* **109**(6): 2630-2633.

Mancini, F., Di Conza, G., Monti, O., Macchiarulo, A., Pellicciari, R., Pontecorvi, A., and Moretti, F. 2010. Puzzling over MDM4-p53 network. *Int J Biochem Cell Biol* **42**(7): 1080-1083.

Marine, J. and Jochemsen, A. 2005. Mdmx as an essential regulator of p53 activity. *Biochemical and Biophysical Research Communications* **331**(3): 750-760.

Marine, J.C., Dyer, M.A., and Jochemsen, A.G. 2007. MDMX: from bench to bedside. *J Cell Sci* **120**(Pt 3): 371-378.

Martinez, L.A., Goluszko, E., Chen, H.Z., Leone, G., Post, S., Lozano, G., Chen, Z., and Chauchereau, A. 2010. E2F3 is a mediator of DNA damage-induced apoptosis. *Mol Cell Biol* **30**(2): 524-536.

Martins, C.P., Brown-Swigart, L., and Evan, G.I. 2006. Modeling the therapeutic efficacy of p53 restoration in tumors. *Cell* **127**(7): 1323-1334.

McClellan, K.A. and Slack, R.S. 2007. Specific in vivo roles for E2Fs in differentiation and development. *Cell Cycle* **6**(23): 2917-2927.

Meletis, K., Wirta, V., Hede, S.M., Nister, M., Lundeberg, J., and Frisen, J. 2006. p53 suppresses the self-renewal of adult neural stem cells. *Development* **133**(2): 363-369.

Migliorini, D., Lazzerini Denchi, E., Danovi, D., Jochemsen, A., Capillo, M., Gobbi, A., Helin, K., Pelicci, P.G., and Marine, J.C. 2002. Mdm4 (Mdmx) regulates p53-induced growth arrest and neuronal cell death during early embryonic mouse development. *Mol Cell Biol* **22**(15): 5527-5538.

Montes de Oca Luna, R., Wagner, D.S., and Lozano, G. 1995. Rescue of early embryonic lethality in mdm2-deficient mice by deletion of p53. *Nature* **378**(6553): 203-206.

Morachis, J.M., Murawsky, C.M., and Emerson, B.M. 2010. Regulation of the p53 transcriptional response by structurally diverse core promoters. *Genes Dev* **24**(2): 135-147.

Murphy, D.J., Junttila, M.R., Pouyet, L., Karnezis, A., Shchors, K., Bui, D.A., Brown-Swigart, L., Johnson, L., and Evan, G.I. 2008. Distinct Thresholds Govern Myc's Biological Output In Vivo. *Cancer Cell* **14**(6): 447-457.

Okamoto, K., Taya, Y., and Nakagama, H. 2009. Mdmx enhances p53 ubiquitination by altering the substrate preference of the Mdm2 ubiquitin ligase. *FEBS Lett* **583**(17): 2710-2714.

Parant, J., Chavez-Reyes, A., Little, N.A., Yan, W., Reinke, V., Jochemsen, A.G., and Lozano, G. 2001. Rescue of embryonic lethality in Mdm4-null mice by loss of Trp53 suggests a nonoverlapping pathway with MDM2 to regulate p53. *Nat Genet* **29**(1): 92-95.

Paulson, Q.X., McArthur, M.J., and Johnson, D.G. 2006. E2F3a stimulates proliferation, p53-independent apoptosis and carcinogenesis in a transgenic mouse model. *Cell Cycle* **5**(2): 184-190.

Polager, S. and Ginsberg, D. 2009. p53 and E2f: partners in life and death. *Nat Rev Cancer* **9**(10): 738-748.

Reed, D., Shen, Y., Shelat, A.A., Arnold, L.A., Ferreira, A.M., Zhu, F., Mills, N., Smithson, D.C., Regni, C.A., Bashford, D. et al. 2010. Identification and characterization of the first small molecule inhibitor of MDMX. *J Biol Chem* **285**(14): 10786-10796.

Ringshausen, I., Oshea, C., Finch, A., Swigart, L., and Evan, G. 2006. Mdm2 is critically and continuously required to suppress lethal p53 activity in vivo. *Cancer Cell* **10**(6): 501-514.

Rowland, B.D., Denissov, S.G., Douma, S., Stunnenberg, H.G., Bernards, R., and Peeper, D.S. 2002. E2F transcriptional repressor complexes are critical downstream targets of p19(ARF)/p53-induced proliferative arrest. *Cancer Cell* **2**(1): 55-65.

Ryan, R.F., Schultz, D.C., Ayyanathan, K., Singh, P.B., Friedman, J.R., Fredericks, W.J., and Rauscher, F.J., 3rd. 1999. KAP-1 corepressor protein interacts and colocalizes with heterochromatic and euchromatic HP1 proteins: a potential role for Kruppel-associated box-zinc finger proteins in heterochromatin-mediated gene silencing. *Mol Cell Biol* **19**(6): 4366-4378.

Sarkisian, C.J., Keister, B.A., Stairs, D.B., Boxer, R.B., Moody, S.E., and Chodosh, L.A. 2007. Dose-dependent oncogene-induced senescence in vivo and its evasion during mammary tumorigenesis. *Nat Cell Biol* **9**(5): 493-505.

Shangary, S., Qin, D., McEachern, D., Liu, M., Miller, R.S., Qiu, S., Nikolovska-Coleska, Z., Ding, K., Wang, G., Chen, J. et al. 2008. Temporal activation of p53 by a specific MDM2 inhibitor is selectively toxic to tumors and leads to complete tumor growth inhibition. *Proc Natl Acad Sci U S A* **105**(10): 3933-3938.

Sherr, C.J. and McCormick, F. 2002. The RB and p53 pathways in cancer. *Cancer Cell* **2**(2): 103-112.

Sun, S.H., Zheng, M., Ding, K., Wang, S., and Sun, Y. 2008. A small molecule that disrupts Mdm2-p53 binding activates p53, induces apoptosis and sensitizes lung cancer cells to chemotherapy. *Cancer Biol Ther* **7**(6): 845-852.

TeKippe, M., Harrison, D.E., and Chen, J. 2003. Expansion of hematopoietic stem cell phenotype and activity in Trp53-null mice. *Exp Hematol* **31**(6): 521-527.

Tsai, S.Y., Opavsky, R., Sharma, N., Wu, L., Naidu, S., Nolan, E., Feria-Arias, E., Timmers, C., Opavska, J., de Bruin, A. et al. 2008. Mouse development with a single E2F activator. *Nature* **454**(7208): 1137-1141.

Uldrijan, S., Pannekoek, W.J., and Vousden, K.H. 2007. An essential function of the extreme C-terminus of MDM2 can be provided by MDMX. *Embo J* **26**(1): 102-112.

Valentin-Vega, Y.A., Okano, H., and Lozano, G. 2008. The intestinal epithelium compensates for p53-mediated cell death and guarantees organismal survival. *Cell Death Differ* **15**(11): 1772-1781.

Vassilev, L.T., Vu, B.T., Graves, B., Carvajal, D., Podlaski, F., Filipovic, Z., Kong, N., Kammlott, U., Lukacs, C., Klein, C. et al. 2004. In vivo activation of the p53 pathway by small-molecule antagonists of MDM2. *Science* **303**(5659): 844-848.

Vazquez, A., Bond, E.E., Levine, A.J., and Bond, G.L. 2008. The genetics of the p53 pathway, apoptosis and cancer therapy. *Nat Rev Drug Discov* **7**(12): 979-987.

Ventura, A., Kirsch, D.G., McLaughlin, M.E., Tuveson, D.A., Grimm, J., Lintault, L., Newman, J., Reczek, E.E., Weissleder, R., and Jacks, T. 2007. Restoration of p53 function leads to tumour regression in vivo. *Nature* **445**(7128): 661-665.

Vousden, K.H. and Lane, D.P. 2007. p53 in health and disease. *Nat Rev Mol Cell Biol* **8**(4): 275-283.

Vousden, K.H. and Prives, C. 2009. Blinded by the Light: The Growing Complexity of p53. *Cell* **137**(3): 413-431.

Wade, M. and Wahl, G.M. 2009. Targeting Mdm2 and Mdmx in cancer therapy: better living through medicinal chemistry? *Mol Cancer Res* **7**(1): 1-11.

Wu, L., Timmers, C., Maiti, B., Saavedra, H.I., Sang, L., Chong, G.T., Nuckolls, F., Giangrande, P., Wright, F.A., Field, S.J. et al. 2001. The E2F1-3 transcription factors are essential for cellular proliferation. *Nature* **414**(6862): 457-462.

Xiong, S., Van Pelt, C.S., Elizondo-Fraire, A.C., Liu, G., and Lozano, G. 2006. Synergistic roles of Mdm2 and Mdm4 for p53 inhibition in central nervous system development. *Proc Natl Acad Sci U S A* **103**(9): 3226-3231.

Xue, W., Zender, L., Miething, C., Dickins, R.A., Hernando, E., Krizhanovsky, V., Cordon-Cardo, C., and Lowe, S.W. 2007. Senescence and tumour clearance is triggered by p53 restoration in murine liver carcinomas. *Nature* **445**(7128): 656-660.

Ziebold, U., Lee, E.Y., Bronson, R.T., and Lees, J.A. 2003. E2F3 loss has opposing effects on different pRB-deficient tumors, resulting in suppression of pituitary tumors but metastasis of medullary thyroid carcinomas. *Mol Cell Biol* **23**(18): 6542-6552.

Zindy, F., Williams, R.T., Baudino, T.A., Rehg, J.E., Skapek, S.X., Cleveland, J.L., Roussel, M.F., and Sherr, C.J. 2003. Arf tumor suppressor promoter monitors latent oncogenic signals in vivo. *Proc Natl Acad Sci U S A* **100**(26): 15930-15935.

Publishing Agreement

It is the policy of the University to encourage the distribution of all theses, dissertations, and manuscripts. Copies of all UCSF theses, dissertations, and manuscripts will be routed to the library via the Graduate Division. The library will make all theses, dissertations, and manuscripts accessible to the public and will preserve these to the best of their abilities, in perpetuity.

Please sign the following statement:

I hereby grant permission to the Graduate Division of the University of California, San Francisco to release copies of my thesis, dissertation, or manuscript to the Campus Library to provide access and preservation, in whole or in part, in perpetuity.

Daniel Garcia 3/24/2011

Author Signature Date